UNIVERSITAT POLITÈCNICA DE CATALUNYA
BARCELONATECH

Escola Tècnica Superior d'Enginyeria
de Telecomunicació de Barcelona

DESIGN OF A WEARABLE DEVICE FOR EVALUATION OF FRAILTY IN OLDER PEOPLE

A Master's Thesis

Submitted to the Faculty of the

Escola Tècnica d'Enginyeria de Telecomunicació de Barcelona

Universitat Politècnica de Catalunya

by

David Hurtado Martínez

In partial fulfilment

of the requirements for the degree of

MASTER IN ELECTRONIC ENGINEERING

Advisor: Javier Rosell Ferrer

Barcelona, October 2017

Title of the thesis

Design of a wearable device for evaluation of frailty in older people

Author

David Hurtado Martínez

Advisor

Javier Rosell Ferrer

Abstract

Frailty in elder people is becoming a major concern with the passage of years because of the world population ageing. The early diagnosis of frailty might be used in the future to prevent and care in a better manner the health of a person, and thus, improve his/her life conditions.

The results of this project are the design of a wearable device to measure grip strength and walk time embedded in an anti-stress ball, the design and implementation of a fast prototype and the design and implementation of a compressive force calibration system.

The presented fast prototype shows that it would be feasible to produce an anti-stress ball able to monitor and diagnose frailty in old people; but, a trial on old people shall be first performed in order to obtain a proper threshold for weak grip strength criterion using the anti-stress ball.

To my family and Laura

Acknowledgements

First of all, I would like to thank my family for all the support that I have received not only along the development of this thesis, but also throughout these seven years at university. Additionally, I feel immensely fortunate to share my achievements and failures with Laura, who has always been ready for whatever may come.

In the scope of this work, I am grateful to Javier Rosell Ferrer for his empathy and advice during the last months. Also, I would like to show my deep gratitude to all professors with whom I have shared a classroom during the last years.

And last but not least, I would like to mention a group of friends who have been a great support from the very beginning of this university adventure. Thank you, Àlex. Than you, Alejandro. Thank you, Clever. Thank you, Luis.

Revision history and approval record

Revision	Date	Purpose
0	04/09/2017	Document creation
1	26/09/2017	Change format. Add system information. Add grip ball calibration results.
2	16/10/2017	Change document structure. Add conceptual and fast prototype design. Add fast prototype implementation. Add project costs.
3	17/10/2017	Add results.
4	18/10/2017	Add conclusions and abstract. Minor changes.

Written by:		Reviewed and approved by:	
Date	18/10/2017	Date	18/10/2017
Name	David Hurtado Martínez	Name	Javier Rosell Ferrer
Position	Project Author	Position	Project Supervisor

Table of contents

List of Figures

List of Tables

1. Introduction

1.1. Statement of purpose

Frailty is a clinical syndrome that affects most of old people. The presence of frailty in an adult increases with advancing age - being more common in women than men – and in lower socio-economic environments. Elderly population with frailty diagnosis are at high risk for major adverse health: disability, falls, hospitalization and mortality.

The seminal work of Linda P. Fried [1] in the identification of a frailty phenotype prevails as one of the popular approaches to diagnose frail in an adult. Fried's phenotype includes the following five criteria:

- Unintentional weight loss
- Self-reported exhaustion
- Muscle weakness assessed by grip strength
- Slow walking
- Low physical activity

In this project, a wearable device will be designed and constructed to measure some of the above listed parameters to check how an individual is evolving. The wearable device is intended to be used by an adult without the supervision of a doctor or professional. Moreover, the device must be a low-cost embedded system with low energy consumption, friendly user interface and reliable measurements.

1.2. Project requirements

The project requirements are listed in Table 1.

Table 1 - Project requirements

#	Description of the requirement
1	Conceptual design of a wearable device:
2	– able to reliable measure some of Fried's frailty criteria.
3	– that can be used by an adult without the supervision of a doctor or a professional.
4	– with the lowest cost possible.
5	– with a low energy consumption.
6	– with a friendly user interface.
7	– battery-operated.
8	– with wireless power transfer charging system.

9	– with wireless communication scheme.
10	– with data persistency.
11	– with a debugging interface for development phase.
12	– with a modular and scalable software architecture.
13	Fast prototype design of the wearable device:
14	– as a proof-of-concept of the conceptual design.
15	– able to reliable measure some of Fried's frailty criteria.
16	– that can be used by an adult without the supervision of a doctor or a professional.
17	– with the lowest cost possible.
18	– with a friendly user interface.
19	– with a debugging interface for development phase.
20	– with a modular and scalable software architecture.
21	Implementation of the wearable device fast prototype:
22	– following the system software architecture.
23	– made of off-the-shelf electronic components.
24	– with the electronic system embedded in the mechanic system.
25	– enables an easy real testing of the system.

1.3. Deviations from the initial plan

During the development of the project, it has been critically necessary to calibrate the Force-Sensing Resistors (FSR). Since there are no measurement devices in the laboratory that could have helped to calibrate a compression force, the project scope had to be modified to include the design and implementation of a deadweight measurement device.

Table 2 - Project requirements from deviations

#	Description of the requirement
26	Design of a deadweight measurement device able to reliable measure a compression force.

27	Implementation of a deadweight measurement device able to reliable measure a compression force.

1.4. Document structure

The document structure consists of the following chapters:

- **Chapter 1** is intended to define the purpose of this work as well as the derived requirements to fulfil the project scope. Also, the deviations from the initial plan are explained.
- **Chapter 2** is intended to introduce the concept of frailty to the reader based on Fried's fraily criterion.
- **Chapter 3** is intended to compile the state-of-the-art related to the measurement of frailty symptoms.
- **Chapter 4** is intended to present the conceptual design of the wearable device.
- **Chapter 5** is intended to present the fast prototype design of the wearable device.
- **Chapter 6** is intended to detail the implementation of the wearable device fast prototype.
- **Chapter 7** is intended to present the design and implementation of the deadweight measurement device.
- **Chapter 8** is intended to highlight the results of this work.
- **Chapter 9** is intended to gather the costs of the overall project as well as the cost of the wearable device fast prototype.
- **Chapter 10** is intended to finally mention the conclusions and future development of this project.

2. Frailty

2.1. Introduction

Frailty is considered to be highly prevalent with increasing age and to confer high risk for adverse health outcomes, including mortality, falls and hospitalization. But there is an absence of a standardized and valid method for screening of those who are truly frail so as to effectively target care.

Potential definitions of frailty abound, defining frailty as synonymous with disability, comorbidity, or advanced old age. There is a growing consensus that markers of frailty include age-associated declines in lean body mass, strength, endurance, balance, walking performance, and low activity, and that multiple components must be present clinically to constitute frailty. Many of these factors are related and can be unified, theoretically, into a cycle of frailty associated with declining energetics and reserve (Figure 1). The core elements of this cycle are those commonly identified as clinical signs and symptoms of frailty.

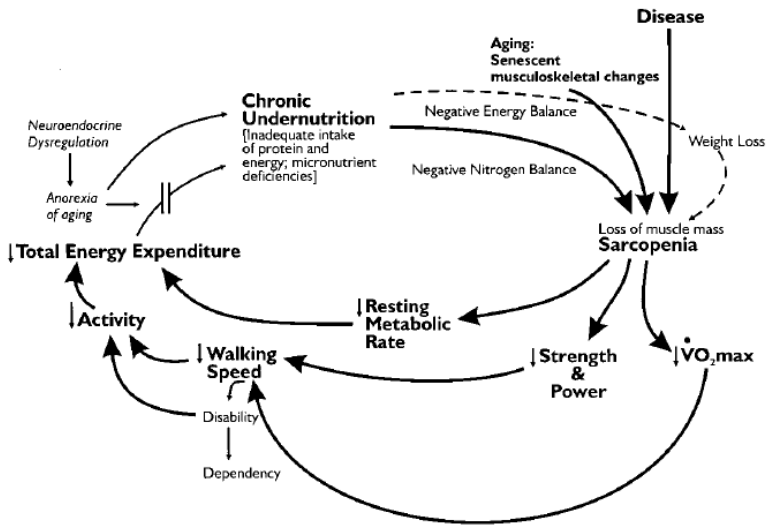

Figure 1 - Cycle of frailty hypothesized as consistent with demonstrated pairwise associations and clinical signs and symptoms of frailty

2.2. Fried's frailty criterion

Linda P. Fried provided a frailty criterion with the potential of standardize the definition of frailty among older adults. The phenotype of frailty includes the following elements: weight loss, weak grip strength, exhaustion, slow walking speed and low physical activity. Fried's criterion specifies that frailty is present when three out of these five characteristics are met in a person.

2.2.1. Weight loss

The way to measure the weight loss is based on the comparison of the weight year to year. If there has been an unintentional difference of more than a 5%, the frailty criterion of weight loss is met.

2.2.2. Exhaustion

The way to measure the exhaustion of the patient is based on the CES Depression Scale. The CESD-R is a screening test for depression and depressive disorder. The CESD-R measures symptoms defined by the American Psychiatric Association' Diagnostic and Statistical Manual for a major depressive episode. The test is composed of 20 statements and, for each phrase, the patient must answer the question “How often in the last week did you feel this way?” with one of the following answers:

1. Rarely or none of the time (< 1 day).
2. Some or a little of the time (1–2 days).
3. A moderate amount of the time (3–4 days), or
4. Most of the time.

In the case of measuring the exhaustion, the following two statements are read.

- I felt that everything I did was an effort.
- I could not get going.

Subjects answering “3” or “4” to either of these questions are categorized as frail by the exhaustion criterion.

2.2.3. Low Physical Activity

Based on the short version of the Minnesota Leisure Time Activity questionnaire, the physical activity is measure by asking about walking, chores (moderately strenuous), mowing the lawn, raking, gardening, hiking, jogging, biking, exercise cycling, dancing, aerobics, bowling, golf, singles tennis, doubles tennis, racquetball, calisthenics, swimming and so on. This way, the total kilocalories expended per week can be calculated using a standardized algorithm.

- A frail man would expend less than 383 kilocalories of physical activity per week.
- A frail woman would expend less than 270 kilocalories of physical activity per week.

2.2.4. Slow Walking Speed

The walking speed criterion is based on a 4.5 meter walk test in which the time is captured. The table below indicates the cut off marks to meet the frailty criteria classified by gender and height.

Table 3 - Slow walking speed criteria for men

Men	***Cut-off for Time to Walk 4.5 meters (15 feet) criterion for frailty***
Height ≤ 173 cm	≥7 seconds
Height > 173 cm	≥6 seconds

Table 4 - Slow walking speed criteria for women

Women	*Cut-off for Time to Walk 4.5 meters (15 feet) criterion for frailty*
Height ≤ 159 cm	≥7 seconds
Height > 159 cm	≥6 seconds

2.2.5. Weak Grip Strength

The grip strength criterion is based on a grip test to capture the kilograms of force that the subject can still apply. It is worth noting that the force unit in the International System (SI) is the Newton (N). However, in this project, the unit for force will be the kilogram of force (kgf): 1 kgf is equivalent to 9.806 N.

The table below indicates the cut off marks to meet the frailty criteria classified by gender and body mass index (BMI).

Table 5 - Weak grip strength criteria for men

Men	*Cut-off for grip strength (Kg) criterion for frailty*
BMI ≤ 24	≤29
BMI 24.1 – 26	≤30
BMI 26.1 – 28	≤30
BMI > 28	≤32

Table 6 - Weak grip strength criteria for women

Women	*Cut-off for grip strength (Kg) criterion for frailty*
BMI ≤ 23	≤17
BMI 23.1 – 26	≤17.3
BMI 26.1 – 29	≤18
BMI > 29	≤21

2.3. Frailty measurement

Current assessments of frailty of older people in hospitals and in private practices are limited in their ability to reflect everyday performance and to evaluate patients' true capabilities in a natural scenario. Numerous researchers have suggested that information technology (IT) and sensor technology - in particular, wearable inertial sensors - are important tools for overcoming these problems.

In this work, the measurement of the grip strength will be the cornerstone.

3. Grip strength

3.1. Introduction

Grip force is identified as a reflection of global muscular capacity, particularly for the elderly where high correlations between grip force and global muscle capacity have been reported. It follows that, as well as measuring muscle capacity, grip force changes can also identify any decrease in capacity, something that would be really useful as part of an evaluation of old people. Therefore, the grip strength is an extremely useful indicator of other clinical conditions that affect the ability of elderly to remain in their own homes, such as frailty and nutritional status.

Grip force has an added advantage compared to other physical capacity tests in that it is completely objective and can be self-administered, without requiring a third person to be present. An automatic grip force device could therefore be used in the home, provided it was autonomous and communicant.

The relationship between grip-strength and frailty makes grip strength measurement one of the key elements of any geriatric evaluation.

The innovations carried out in recent years in the field of grip-strength measurement have been poor. The most usual way to carry out this specific test is by using hand-grip and pinch-force dynamometers. Although these dynamometers are highly reliable and highly accurate, they are all designed for use by a trained evaluator, something that is not possible for home-based functional evaluation

3.2. State-of-the-art

3.2.1. Jamar

The “gold-standard” grip-strength dynamometer, according to the American Society of Hand Therapists (ASHT) is the Jamar [3]. As seen in Figure 2, the handle of the dynamometer is placed at the second handle position. Subjects are placed in a chair facing the evaluator, with their feet flat on the floor, their back straight and placed against the back of the chair. The subject’s arms are pressed against their body, with the shoulder abducted and the elbow flexed to 90°. All tests are executed with the dominant hand and the maximal grip-strength is measured (Figure 3) over three attempts with a two-minute rest between trials.

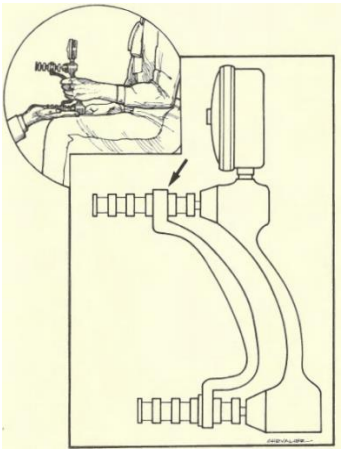

Figure 2 - Grip strength measurement with Jamar dynamometer

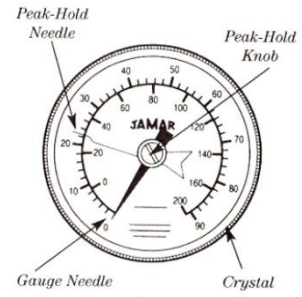

Figure 3 - Jamar dynamometer display: 90 kilograms maximum reading

3.2.2. Datagrip

DataGrip [4] is a grip-strength measurement tool intended for small infants. As shown schematically in Figure 4, the system is composed of a round bar grip measurement device containing two small pressure sensors, a sensor interface and a personal computer. The sensor interface includes a strain-gauge transducer that enables the expression of the measurement in terms of force, pressure, acceleration, or displacement. The DataGrip pressure is input to the sensor interface as analog voltage from the two small pressure sensors via a shielded cable. The strain data from the sensors are converted to pressure (MPa) by control software supplied by the sensor interface.

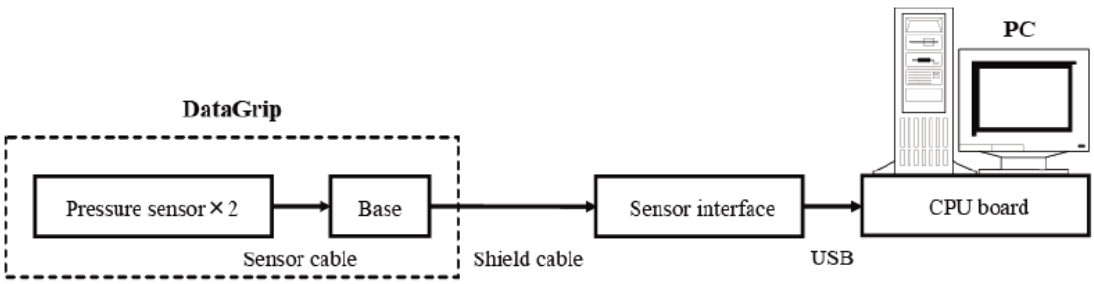

Figure 4 - Schematic of the DataGrip environment

The DataGrip is a cylindrical bar (Figure 5) with a diameter of 15 mm, 75 mm long and weighs 50 grams. The aluminum round bar consists of up-and-down grip shafts. A silicon tube encases the entire pressure-sensitive span of 50 mm. To measure the grip strength, the hand grasps the round bar wrapped with silicone tube. Two small pressure sensors of 6 mm diameter are bonded between up-and-down grip shafts with a special adhesive.

The sensor cable of the pressure sensors passes through a slot in the down shaft to a component base attached to the down grip shaft. The signal lines of the sensor cable are connected at the base to a shielded cable clamped to the same shaft.

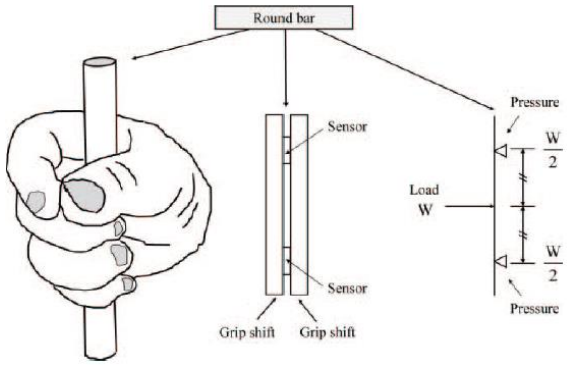

Figure 5 - Details of the DataGrip round bar

There is a newer version of the initial DataGrip, the DataGrip II; which is the result of an improvement of the DataGrip in the following four aspects:

1. The sensor is changed from a compact pressure sensor to an ultra-compact compression load cell to improve the response performance.
2. The diameter of the round rod is decreased by 2 mm, which makes it easier to grip.
3. The connection of the data lead in the cable between the grip strength measuring device and sensor interface is changed from a cable clamp to a connector plug to improve the durability and give it aesthetic appeal.
4. Its appearance is changed from a silicon tube to a stuffed toy with the intention of stimulating the interest of infants to try to attract them to the measuring device.

3.2.3. Sensorized glove

The purpose of sensorized glove [5] (Figure 6) is to measure the maximum isometric strength of the hand and forearm muscles. The whole system architecture is composed of three main building blocks:

- Sensorized glove: this glove is equipped with five sensors, which are attached to it.
- Hardware device: it consists of a tiny electronic circuit, protected by a case specifically designed for it. Its main functions are the acquisition and processing of the signals coming from the sensors, and transmitting them to the PC via the USB connection.
- PC application: the third component of the system architecture is in charge of receiving the data sent by the hardware device via the USB connection, and storing and visualizing them, using a graphical user interface.

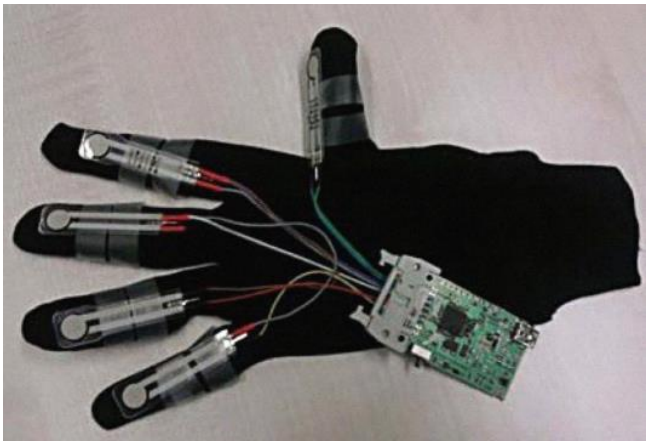

Figure 6 - Sensorized glove from [5]

The sensors used in this work have been Force Sensitive Resistors (FSR) manufactured by Tekscan (Figure 7).

Figure 7 - Tekscan FSR sensor

Another type of sensorized glove [11] is shown in Figure 8. The microcontroller unit on the main board retrieves the data from seveteen 9-axis inertial IMU sensors and the voltage from the Interlink Electronics' force sensitive resistors on each finger.

Figure 8 - Sensorized glove from [11]

3.2.4. Domo-Grip

The Domo-Grip system [6] consists of three components: the Grip-Ball, the Grip-Box, and the Grip-Soft. The Grip-Ball is the dynamometer used to measure grip force, while the Grip-Box enables the communication between the dynamometer and the user. The Grip-Soft is an interactive software suite designed for both patients and clinical supervision.

The aim of the Domo-Grip project is to allow any non-trained person measure the grip strength by means of an easy-to-use and comfortable dynamometer. Most of the

dynamometers are rigid, such as the gold standard Jamar, and can therefore be painful for old subjects with fragile skin, which could modify the grip-strength test results. Given that the grip strength test requires a maximum voluntary contraction, the use of a comfortable dynamometer could encourage subjects to exert a maximal contraction. The Grip-ball consists of an airtight, flexible, inflatable plastic ball containing pressure and temperature sensors, a digitization function, and a communication system (Figure 9). The Grip-ball transmits the pressure measured by the sensor inside the ball in real time when the ball is squeezed. The pressure applied is proportional to the force exerted by the user.

The electronic circuit, which measures 45 mm in diameter, and 30 mm in height (Figure 9), is fixed to the internal part of the Grip-ball. It is equipped with a pressure sensor (MS5535C), which has a measurement range of 0–1.400 kPa and a 15-bit ADC conversion. The sensor is managed by a controller (PIC 18LF13K22 Microchip transmitter Bluetooth ARF32), which acquires the sensor data, and transmits them via Bluetooth to a either a mobile phone or a tablet.

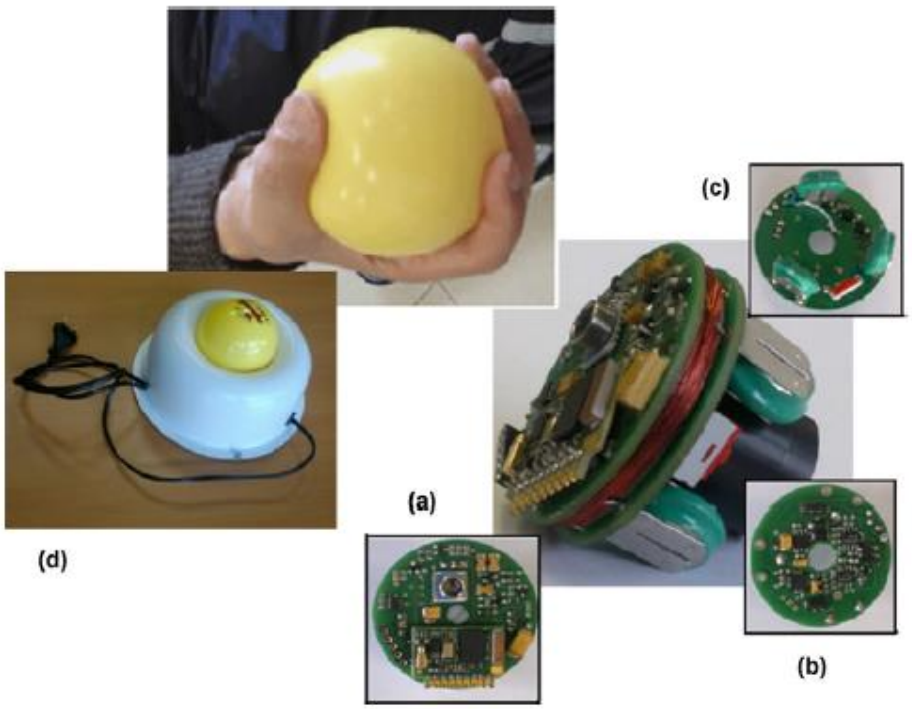

Figure 9 - The Grip-ball and its internal electronics: (a) sensor and communication modules; (b) sensor side; (c) battery side; (d) the Grip-ball in its recharging base

Two prototype devices were developed, each with a different power supply design. The first makes use of standard 1100-mAh batteries, allowing a continuous transmission for a 36-hour period. But, such a system is not practical since the electronic components required to measure and transmit the pressure signal must be kept inside the ball. That is why a reed switch was used to disconnect the battery from the electronic circuits when the ball was not in use. The switch can be turned off by placing the ball in a support base containing a magnet, which turns the reed switch off.

The second prototype [13] includes a rechargeable system to increase the autonomy of the device. The recharging of these batteries is performed using wireless inductive

coupling between the base (including the primary coil and the associated electronics) and the ball where the secondary coil is inserted, along with the battery load electronics.

3.2.5. Portable handgrip device

The proposed system [7] is composed of a sensing handgrip device equipped with a force sensor in order to collect the time-varying muscle controllability of patients (Figure 10) and the software system that visualizes the examination and stores the results in the database.

The two cylinders bridged by the black plastic (Part C in Figure 10) can be moved along the sideline (Part B in Figure 10) such that patients can grasp the device. The movable component of the handgrip device is bound to the fork-like side (Part A in Figure 10) of the device by a rubber band. Patients can use rubber bands of different tension forces in order to customize the maximum squeeze force in the handgrip device. Finally, a FSR force sensor from Interlink Electronics is attached to Part D in Figure 10 to measure the force generated by the grasping action.

The FSR sensor is used in the proposed system because it responds accurately and precisely to the general range of handgrip force and it shows good performance in terms of robustness.

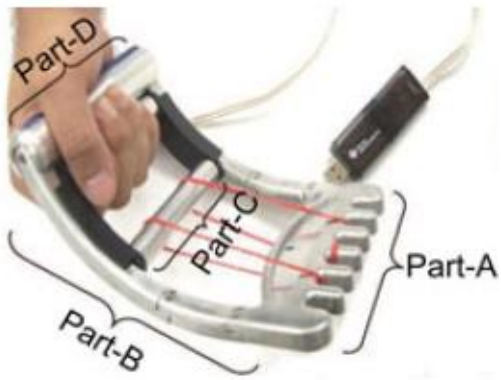

Figure 10 - Portable handgrip device

3.2.6. Tip force

As a simple method to diagnose Sarcopenia, some studies proposed measurement of hand gripforce. But in [9], a development of a force sensor fixed on the surface of the finger to measure the daily motion is proposed. The sensor is required to have repeatability and accuracy which are enough to measure some daily motions. For satisfying both of them, a 8-mm strain gauge-based sensor from Kyowa Electronic Instruments is used (Figure 11).

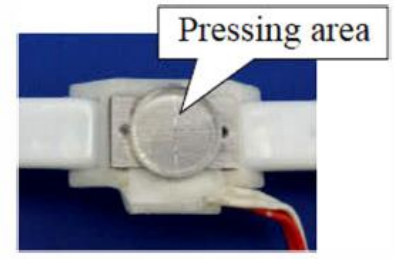

Figure 11 - Strain gauge sensor

3.2.7. Walker device

The measurement principle used to measure the unbalance degree of the forces applied by the walker user on the mobility device [10] [15] is based on the evaluation of the centroid coordinates of the forces that are applied on the walker legs and on the walker hand grips where FSR sensors are placed (Figure 12).

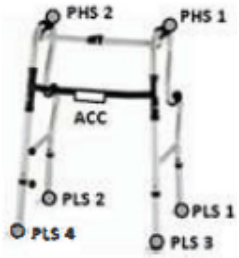

Figure 12 - Four legs walker device with the distribution of FSR sensors

In order to avoid saturation of the sensors that affect seriously the dynamic response, their linearity and their sensitivity, a cylindrical bumper, with an appropriate thickness and stiffness, and a diameter equal to the FSR sensing area, was inserted between the sensor and the surface where the force is applied. The main characteristics of the FSR sensor include a measuring force range of 45 Kg, a linearity error lower than 3% and repeatability better than 2.5% of full scale.

3.2.8. Sole sensors

In [11], a novel system for the monitoring of gait of patients affected by Parkinson disease is proposed. An insole (Figure 13) with embedded FSR sensors allows to capture and analyse the gait over long periods of time and while the patient interacts with non-controlled environments.

The FSR sensors selected in this project are from Tekscan because of the high sensitivity they have and the wide force range.

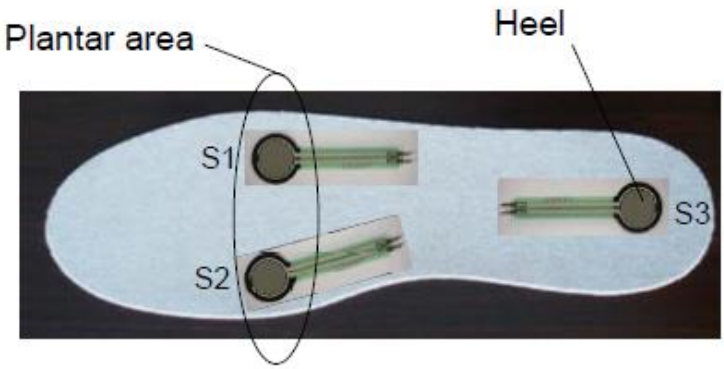

Figure 13 - Insole FSR sensors from [11]

In [14], another sole pressure measurement system is presented to measure the sole pressure and pose of sole in gait motion for Sarcopenia-diagnosed patients. The proposed system has one gyroscope sensor and seven Interlink Electronics' FSR sensors in one sole.

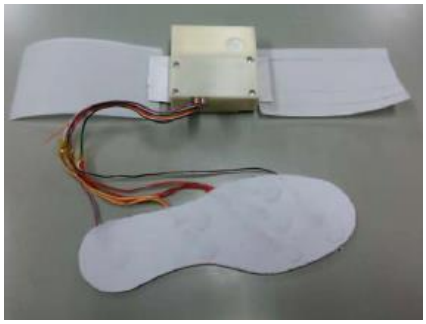

Figure 14 - Insole FSR sensors from [14]

4. Wearable device: conceptual design

The purpose of this section is to present the conceptual design of the wearable device to fulfil the requirements listed in Table 7.

Table 7 - Requirements of the conceptual design

#	Description of the requirement
1	Conceptual design of a wearable device:
2	– able to reliable measure some of Fried's frailty criteria.
3	– that can be used by an adult without the supervision of a doctor or a professional.
4	– with the lowest cost possible.
5	– with a low energy consumption.
6	– with a friendly user interface.
7	– battery-operated.
8	– with wireless power transfer charging system.
9	– with wireless communication scheme.
10	– with data persistency.
11	– with a debugging interface for development phase.
12	– with a modular and scalable software architecture.

The whole system is embedded in a regular anti-stress ball with a size that enables both the integration of all the electronics and eases its manipulation and transport. The wearable device is aimed to be able to measure the following frailty indicators:

- Grip strength (Fried's indicator)
- Sit-to-stand time (alternative indicator)
- Stand-to-sit time (alternative indicator)
- Walk time (Fried's indicator)

The user switches between measurement modes by pressing the ball and once the desired mode is selected, the wearable device starts measuring. The system finishes the current measurement, and transitions to standby mode, when the anti-stress ball is shaken. This basic operation totally matches with the target users, who tend to be old persons reluctant of complicated user interfaces.

The wearable device can be in six different modes that are explained in Table 8.

Table 8 - Modes of operation

Mode	Description of mode
Standby	In this mode, the wearable device has most of the peripherals and external chips in standby mode until the user presses the ball. This way, the battery lifetime is extended due to the low power consumption.
Grip strength	In this mode, the wearable device starts measuring the pressure applied to the anti-stress ball for 5 seconds and stores the highest value of the grip strength into the non-volatile memory. Figure 15 shows a representation of this mode: when the mode is selected by pressing the anti-stress ball (step 1), the system starts acquiring the force applied (step 2); after 5 seconds, the user must shake the wearable device to return to standby (step 3).
Sit-to-stand	In this mode, the wearable device measures the time it takes to the user to go from a sitting position to a standing position and stores it into the non-volatile memory. Figure 16 shows a representation of this mode: when the mode is selected by pressing the anti-stress ball in a sitting position (step 1), the system starts a timer that stops when the user is in a standing position and shakes the wearable device (step 2); consequently, the system returns to standby.
Stand-to-sit	In this mode, the wearable device measures the time it takes to the user to go from a standing position to a sitting position and stores it into the non-volatile memory. Figure 17 shows a representation of this mode: when the mode is selected by pressing the anti-stress ball in a standing position (step 1), the system starts a timer that stops when the user is in a sitting position and shakes the wearable device (step 2); consequently, the system returns to standby.
Walk time	In this mode, the wearable device measures the time it takes to the user to travel a 4.5-meter distance and stores it into the non-volatile memory. Figure 18 shows a representation of this mode: when the mode is selected by pressing the anti-stress ball in a standing position (step 1), the system starts a timer that stops when the user has walked 4.5 meters and shakes the wearable device (step 2); consequently, the system returns to standby.
Data synchronization	In this mode, the wearable device transmits the data stored in the non-volatile memory to an external device (if present) over the wireless communication link. Once this mode is selected

and the data is correctly synchronized, the user must shake the wearable device to return to standby.

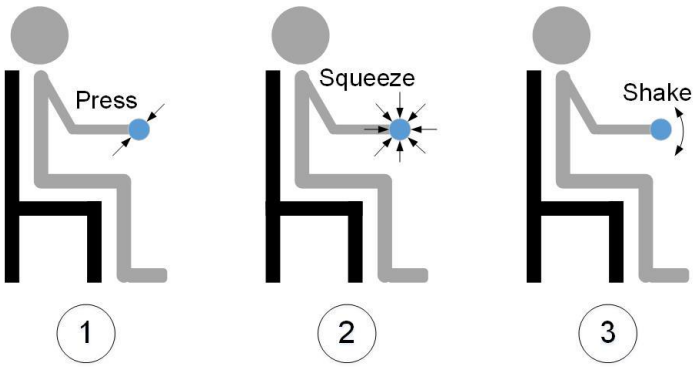

Figure 15 - Grip strength mode representation

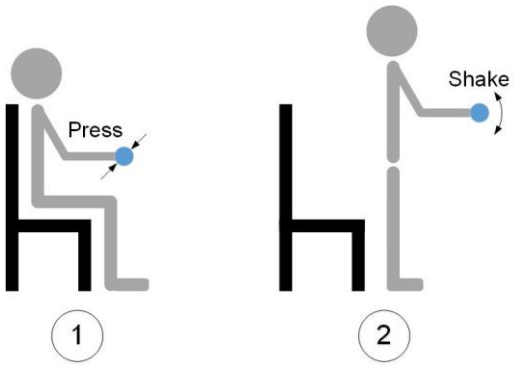

Figure 16 - Sit-to-stand mode representation

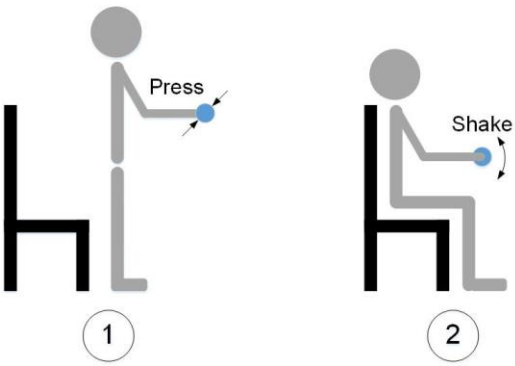

Figure 17 - Stand-to-sit mode representation

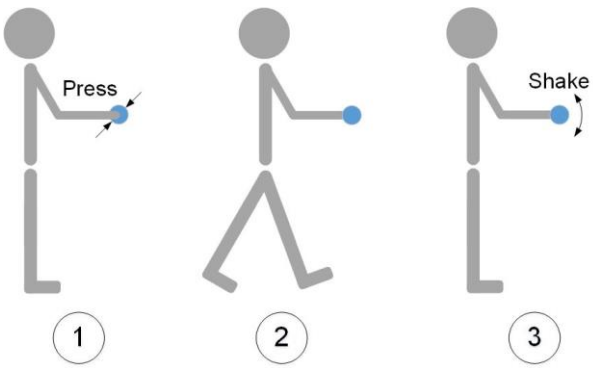

Figure 18 - Walk time mode

4.1. Hardware architecture

The measurement of the grip strength is based on a Force-Sensitive Resistor (FSR) and the measurement of movement, on an accelerometer. The output of these sensors is going to be processed by a microcontroller unit (MCU), which stores the extracted information in a flash memory.

The communication with the outer world is handled through a wireless Bluetooth link. But, for the development stage, a wired serial communication is enabled to debug the system behaviour.

The MCU is also in charge of interfacing with the patient by means of an RGB LED, which will indicate the user in which state of operation is the wearable device.

Finally, the whole system is powered by a battery that is charged through a wireless charging station using a Wireless Power Transfer (WPT) link. The block diagram of the wearable device is shown in Figure 19Figure 19 - System block diagram.

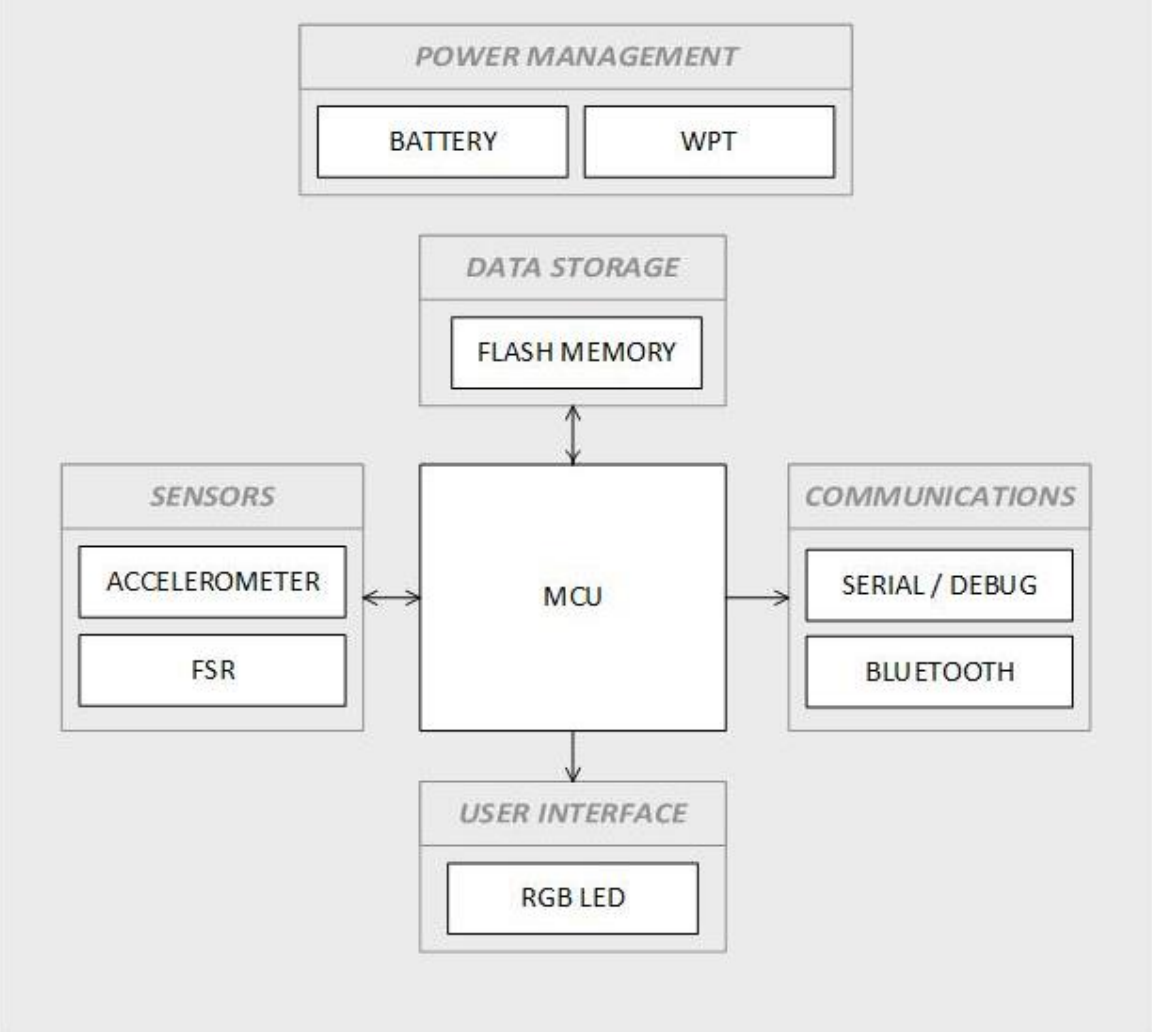

Figure 19 - System block diagram

4.1.1. Microcontroller unit

The microcontroller unit chosen for the wearable device is Microchip's PIC24FJXXXGA204 (Figure 20) because it is a 16-bit microcontroller featuring extreme

low-power management options, 8-MHz internal oscillator, 13-channel ADC, five external interrupts, five 16-bit timers, hardware real-time clock/calendar, three SPI modules and four UART modules among others. There are also 35 I/O pins that can be remapped to any hardware module.

The PIC24FJXXXGA204 is powered with 3.3 V and allows different power-saving modes that would help to fulfil the low-energy consumption requirement.

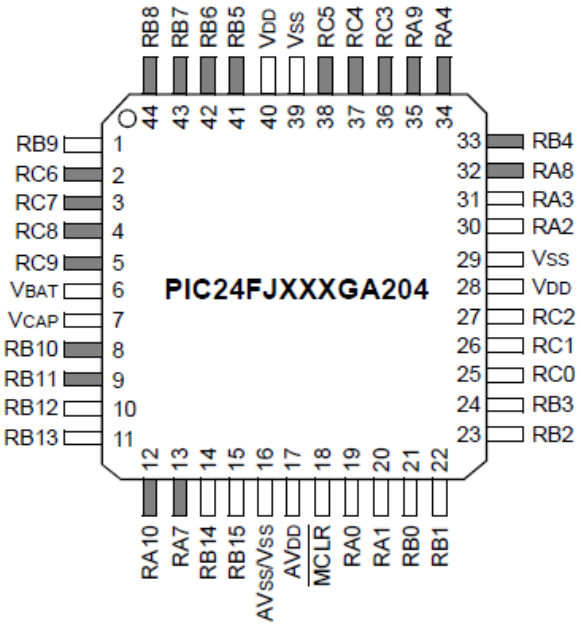

Figure 20 - PIC24FJXXXGA204 pin diagram

4.1.2. Sensors

4.1.2.1. Force-Sensing Resistor

The FSR sensor chosen for this project is the model 402 from Interlink Electronics. An FSR consists of two membranes separated by a thin air gap (Figure 21). The air gap is maintained by a spacer around the edges and by the rigidity of the two membranes. One of the membranes has two sets of inter-digitated fingers that are electrically distinct, with each set connecting to one trace on a tail. The other membrane is coated with FSR ink. When pressed, the FSR ink shorts the two traces together with a resistance that is inversely proportional to the applied force.

Around the perimeter of the sensor, there is a spacer adhesive that serves both to separate the two substrates and hold the sensor together. This spacer may be screen printed of a pressure sensitive adhesive, may be cut from a film pressure sensitive adhesive, or may be built up using any combination of materials that can both separate and adhere to the two substrates.

The conductive traces are typically screen printed from silver polymer thick film ink. However, these traces may also be formed out of gold plated copper as on flexible or standard circuit boards.

One of the exterior surfaces typically includes a mounting adhesive layer to allow mounting to a clean, smooth, rigid surface.

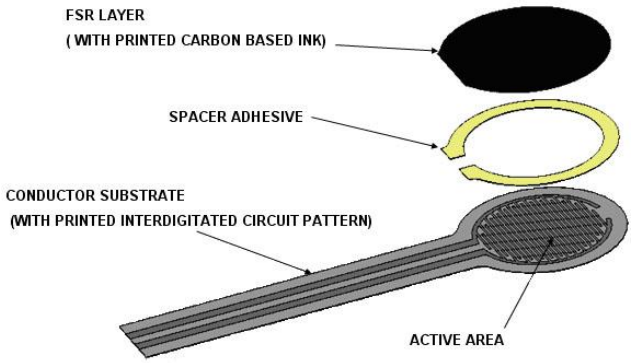

Figure 21 - FSR sensor

A typical resistance-force characteristic curve for an FSR sensor is shown in Figure 22. The "actuation force" – or turn-on – is defined as the force required to bring the sensor from open circuit to below 100 kΩ resistance. This force is influenced by the substrate and overlay thickness and flexibility, size and shape of the actuator, and spacer-adhesive thickness. Immediately after turn-on, the resistance decreases very rapidly. At slightly higher and then intermediate forces, the resistance follows an inverse power law. At the high forces the response eventually saturates to a point where increases in force yield little or no decrease in resistance. Saturation can be pushed higher by spreading the applied force over a larger actuator.

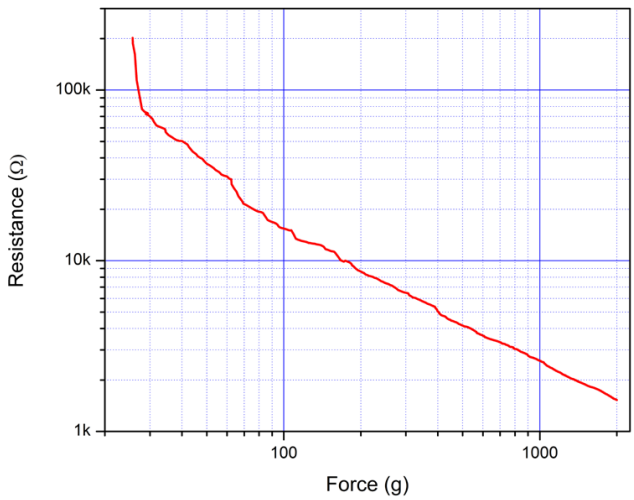

Figure 22 - FSR resistance-force characteristic curve (Interlink's 402 sensor)

The electronic interface of the FSR sensor has been chosen to obtain a linear relationship between the applied force and the output. To do so, the output of the conditioning circuit shall be inversely proportional to the resistance to compensate the inversely proportional relation of the applied force with the resistance of the FSR.

A well-suited topology to implement this inverse proportion is the current-to-voltage converter (Figure 23). But, it needs to be considered that no negative voltage is going to be present in the wearable device. The output voltage is obtained with the following relationship:

$$V_{OUT} = V_{REF} \cdot \left(1 + \frac{R_F}{R_{FSR}}\right)$$

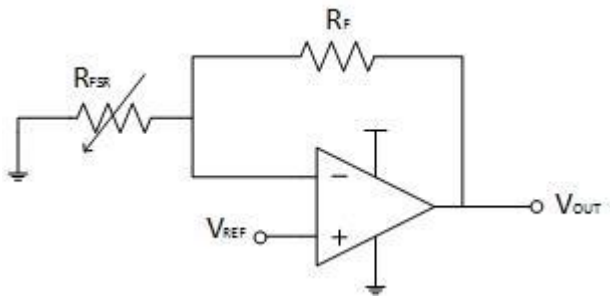

Figure 23 - Current-to-voltage converter

This FSR sensor saturates at 20 N, meaning that it will no longer exhibit a change in resistance above 20 N. However, the sensor will not be damaged at forces greater than 20 N. One possible way to use this sensor at larger forces would be to use any type of foam in the mechanical stack which would dampen the force and reduce the force which the sensor sees. The thicker the soft material, the less force will be transferred to the sensor.

Since the maximum cut-off for grip-strength criterion for frailty is 32 Kgf according to [1], the sensors shall be able to measure above this threshold and with a resolution of tenths of kilograms of force. A reasonable saturation limit for the FSR sensor would be 40 Kgf, well above the aforementioned maximum cut-off. Since one Kilogram of force is equivalent to 9.806 Newtons of force, the FSR shall saturate around 392 N.

$$40\ Kgf \cdot \frac{9.806\ N}{1\ Kgf} = 392.24\ N$$

Therefore, the foam material damping properties and its physical dimensions shall be able to absorb the force applied to the foam so that the 392 N become 20 N at the surface of the FSR sensor.

4.1.2.2. Accelerometer

For this project, the off-the-shelf accelerometer MMA7455 (Figure 24) has been chosen. This sensor covers the needs of the wearable device by far since it has a selectable acceleration range (2g, 4g and 8g) and it can recognize diverse motions (freefall, vibration and pulse). Also, the MMA7455 features a standby mode aimed at battery-operated systems as the one designed in this project. Finally, the communication with the accelerometer can be done either by SPI or I2C, which eases the integration of the sensor into the system.

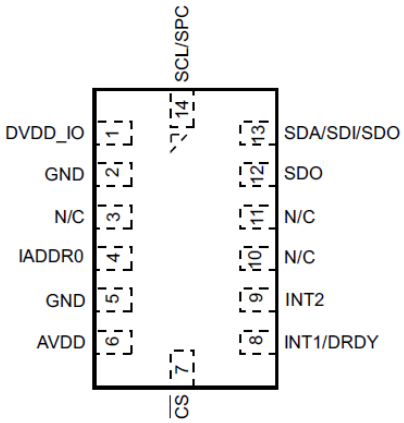

Figure 24 - MMA7455 pin diagram

The MMA7455 is a surface-micromachined integrated-circuit accelerometer. The device consists of a surface micromachined capacitive sensing cell (g-cell) and a signal conditioning ASIC contained in a single package. The g-cell is a mechanical structure formed from semiconductor materials (polysilicon) using semiconductor processes (masking and etching). It can be modelled as a set of beams attached to a movable central mass that move between fixed beams. The movable beams can be deflected from their rest position by subjecting the system to acceleration (Figure 25).

As the beams attached to the central mass move, the distance from them to the fixed beams on one side will increase by the same amount that the distance to the fixed beams on the other side decreases. The change in distance is a measure of acceleration. The g-cell beams form two back-to-back capacitors (Figure 25). As the centre beam moves with acceleration, the distance between the beams changes and each capacitor's value will change. The ASIC uses switched capacitor techniques to measure the g-cell capacitors and extract the acceleration data from the difference between the two capacitors. The ASIC also signal conditions and filters (switched capacitor) the signal, providing a digital output that is proportional to acceleration.

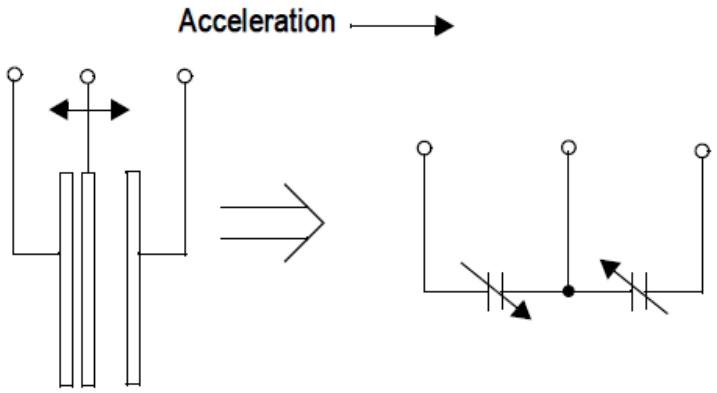

Figure 25 - Accelerometer transducer physical model

4.1.3. Communications

4.1.3.1. Serial / Debug

Since the wireless communication is not available during the development process, it has been required to enable a second data link to debug and test the system. The most common choice for debugging is the serial communication. In this case, the PIC24FJXXXGA204 features four UART modules, so one of these modules is used for the serial link.

The wearable device only transmits data of the system during the development process; therefore, the serial communication consists of a single wire connecting the output of the UART module of the MCU and the outer world.

The UART (Universal Asynchronous Receiver-Transmitter) uses TTL technology to represent bits along with the protocol shown in Figure 26. Basically, a start-bit (logical 0) and a stop-bit (logical 1) determine the beginning and the end of the transmission. In TTL, logical 0 means zero voltage; whereas logical 1, power supply voltage.

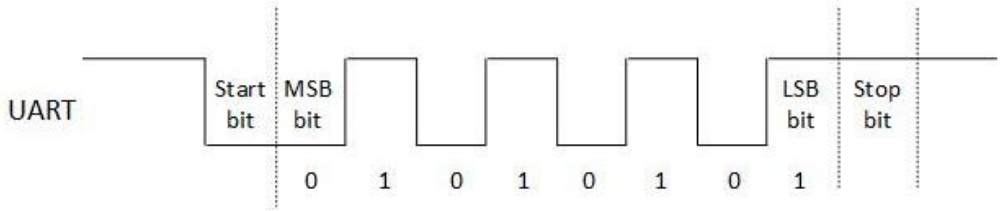

Figure 26 - UART operation: 8-bit transmission of 0x55

Due to the absence of clock line, the transmitter and the receiver shall be configured with the same baud rate; otherwise, the communication will fail.

The most feasible way to visualize the information sent by serial line of the MCU is to print it in a computer monitor. However, personal computers do not have an UART input port. To overcome this issue, the UART interface shall be adapted to any common interface of personal computers (i.e. USB, RS-232). In this case, a USB to TTL adapter will suffice to build the serial communication.

The CP2102 from Silicon Labs (Figure 27) is a single-chip USB-to-UART bridge that provides a simple solution for updating UART designs to USB using a minimum number of components and PCB space. Silicon Labs also offers Virtual COM Port (VCP) device drivers that allow the CP2102 product to appear as a COM port in personal computers.

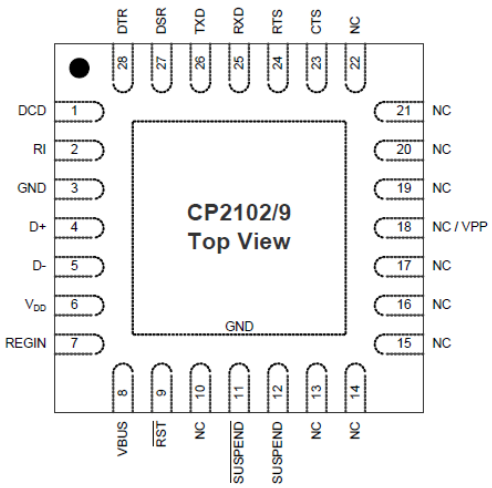

Figure 27 - CP2102 pin diagram

4.1.3.2. Bluetooth

Bluetooth is the chosen wireless communication because it is widely-used in all kind of portable devices, which reduces compatibility issues. Additionally, the technology Bluetooth Low Energy (BLE) fits with the requirement of the low-energy consumption of the wearable device under design.

The module included in the design is the fully-certified BLE BM71BLES1FC2 by Microchip (Figure 28). This module includes the BLE RF transceiver and a certified Bluetooth 4.2 BLE software stack. The BM71 is designed to work with a host MCU that controls its behaviour over a UART interface, and thus generating flexible BLE-based functionality to the wearable device.

In addition to the BLE-related functionality, the module provides a peripheral and general I/O functionality, which can be controlled by using the applicable commands over the UART interface.

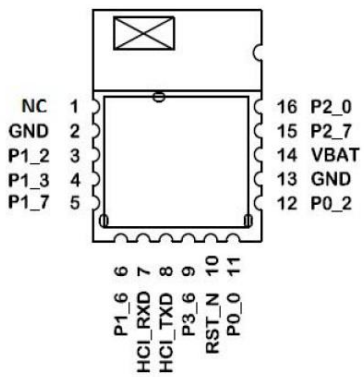

Figure 28 - BM71BLES1FC2 pin diagram

4.1.4. User interface

The user interface of the wearable device shall show the current state of the system in the clearest way possible to the patient. To do so, it has been decided to use an RGB LED because it enables multiple colour codes in a single component. Depending of the

colour, the patient will know, for instance, what kind of measurement is going to be taken or whether the wearable device is running or not.

The colour code for the wearable device is shown in Table 1Table 9.

Table 9 - Wearable device user interface

LED RGB state	Wearable device state
Off	Standby
Red	Grip strength mode
Yellow	Sit-to-stand mode
Blue	Stand-to-sit mode
Green	Walk time mode
White	Data synchronization mode

4.1.5. Data storage

Since the measurements taken throughout the period of usage of the wearable device must be stored, it is totally required to include in the design a data persistency block. The 512-kbit SPI serial flash memory SST25VF512 (Figure 29) by Microchip fulfils the requirements of this project.

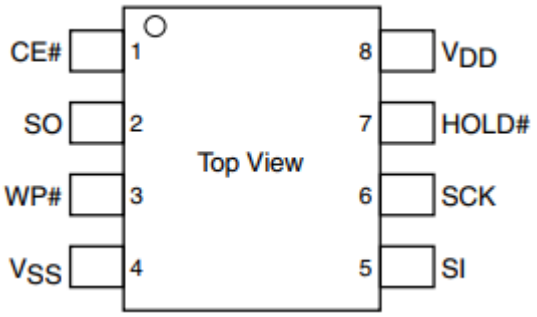

Figure 29 - SST25VF512 pin diagram

4.1.6. Power management

4.1.6.1. Battery

The autonomy of the system depends on the integration of a rechargeable battery that has enough capacity to supply the wearable device during the day. Since the system is always in standby, except in those certain moments of data acquisition, there is not going to be a highly power demand. This fact relaxes the requirements of the battery capacity.

To know what capacity needs the battery of the system, it is first required to approximate the current consumption of the wearable device. Tables below summarizes the current consumption of the wearable device both in full operation and in standby.

Table 10 - Wearable device current consumption: full operation

Module	Full operation	Conditions
PIC24FJXXXGA204	7.6 mA	3.3V, f_{OSC}= 32 MHz.
FSR sensor	170 µA	Assuming that the most consuming component of the circuitry would be the Operational Amplifier MCP6273.
MMA7455 accelerometer	400 µA	Operation mode.
CP2102 USB-to-UART bridge	20.2 mA	Normal operation, V_{REG} enabled.
BM71BLE Blueetooth	10 mA	Peak Tx mode at 3V, Tx=0 dBm. Or, peak Rx mode at 3V.
RGB LED	25 mA	The RGB LED are controlled by GPIO pins of PIC24FJXXXGA204, which are limited to 25 mA.
SST25VF512 Flash Memory	30 mA	Program/Erase current.
TOTAL	93.37 mA	

Table 11 - Wearable device current consumption: standby

Module	Standby	Conditions
PIC24FJXXXGA204	18 µA	3.3V, Sleep mode, T=25ºC.
FSR sensor	170 µA	Assuming that the most consuming component of the circuitry would be the Operational Amplifier MCP6273.
MMA7455 accelerometer	2.5 µA	Standby mode.
CP2102 USB-to-UART bridge	280 µA	Suspended, Bus powered, V_{REG} enabled.
BM71BLE Blueetooth	2.9 µA	Shutdown mode.
RGB LED	0	The RGB LED are controlled by GPIO pins of PIC24FJXXXGA204.
SST25VF512 Flash	15 µA	Standby current.

Memory		
	TOTAL	488.4 µA

The wearable device is not designed to set all the components at full operation at the same time: for instance, the Bluetooth module is not going to be transmitting packets at the same time as the MCU is programming the flash memory. However, as a worst-case value, a current consumption of 93.37 mA is taken for full operation.

On the contrary, the wearable device is indeed designed to be at standby most of the time; therefore, the current consumption of 488.4 µA is taken for standby.

A likely scenario of usage for the system would be 30 minutes of full operation – taking some measurements, writing them in flash memory and synchronizing them wirelessly – and the rest of the day in standby. Hence, the capacity (C) required by the battery would be 58.16 mAh.

$$C = 93.37\ mA \cdot 0.5\ h + 488.4\ \mu A \cdot 23.5\ h = 58.16\ mAh$$

Also, the battery shall have a nominal voltage slightly higher than the 3.3 V power lines, small dimensions and light.

Based on these requirements, the rechargeable battery LP-402025-IS-3 by BAK (Figure 30) has been selected because it has a capacity of 165 mAh (three times bigger than the required), the nominal voltage is 3.7 V, its dimensions are small enough (20x26x3.8 mm) for a regular 7-cm anti-stress ball and it only weighs 4 grams.

Figure 30 - LP-402025-IS-3 3.7 V 165 mAh rechargeable battery

4.1.6.2. Wireless Power Transfer

Since the wearable device is totally enclosed into the anti-stress ball, a wireless power transfer link shall be designed. In this sense, there already exist in the market a lot of charging stations for mobile phones; therefore, the design of the charging station would be out of the scope.

However, the main problem when designing the wireless power transfer is that the antenna in the anti-stress ball may need to be placed at the centre of the sphere; meaning that, there may be too much space between the transmitter and the receiver antenna, worsening this way the coupling factor.

4.2. Software architecture

The software architecture of the wearable device shall be modular and scalable. This means that the design will be able to support the addition of future features without incurring in higher costs in terms of development and integration. Figure 31 presents the software architecture of the system.

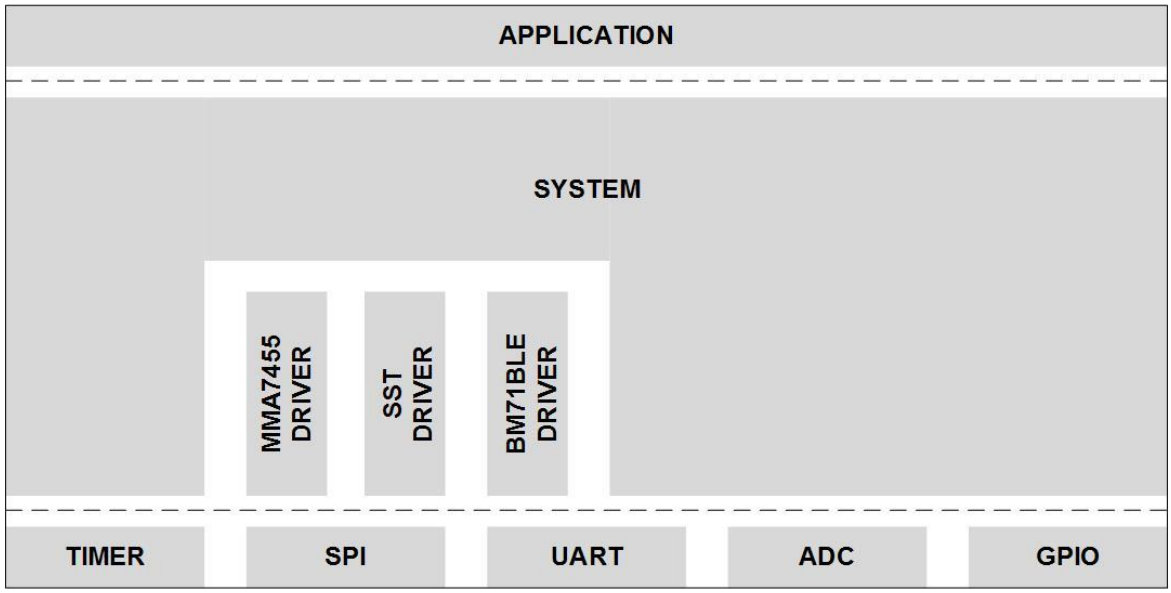

Figure 31 - Software architecture: conceptual design

The meaning of each of the modules in the software architecture is explained in Table 12.

Table 12 - Software modules description

Module	Description of the module
Application	The Application module handles the high-level operation of the wearable device such as state transitions.
System	The System module is the brain of the system since it configures all the peripherals of the MCU and acts as an interface between the Application and the drivers of the external chips (MMA7455, SST and BM71BLE).
MMA7455 Driver	The MMA7455 Driver handles the configuration and correct operation of the external MMA7455 chip.
SST Driver	The SST Driver handles the configuration and correct operation of the external SST25VF512 chip.
BM71BLE Driver	The BM71BLE Driver handles the configuration and correct operation of the external BM71BLE chip.
Timer	The Timer module is used by the system to perform delays during the execution of the system.
SPI	The SPI module is used by the MMA7455 Driver and SST Driver to physically interface with the external chips.
UART	The UART module is used by the BM71BLE Driver and the system to physically interface with the external chips or PC.

ADC	The ADC module is used by the system to sample the state of the input analogue channels such as the output voltage of the FSR's conditioning circuit.
GPIO	The GPIO module is used by the system to interact with different hardware components such as the RGB LED or external chips.

The workflow of the embedded software is detailed in the diagram of Figure 32. After Power-on-Reset, the system is initialized. This means that all the communication interfaces are configured, system variables are reset to a known value and the external devices are prepared for its proper use. After the initialization phase, the system remains in standby mode until the user presses the ball, transitioning this way the wearable device to the grip strength mode and turning on the RGB LED to red colour. At this point, a 5-second timer is started, if the user does not press the ball, the RGB LED will blink each half second until the 5-second timeout occurs and thus starting the grip strength measurement. If, on the contrary, the user presses the anti-stress ball within the 5-second count, the system moves to the next mode – in this case, the sit-to-stand mode – starting the aforementioned process again.

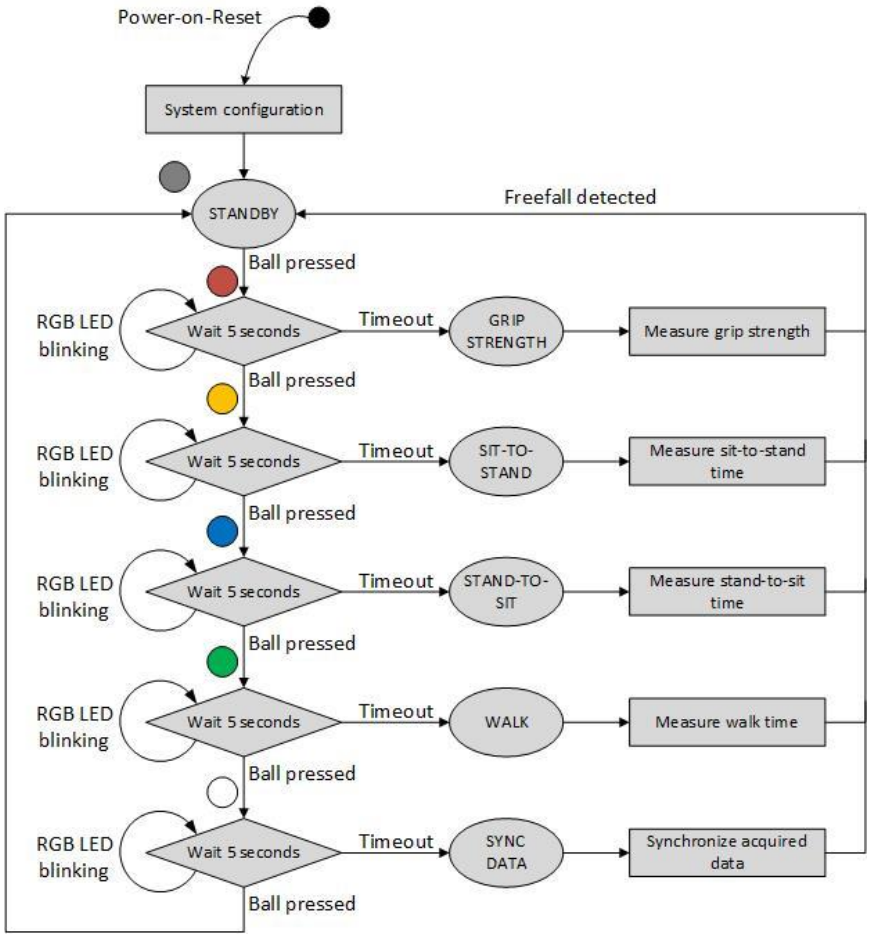

Figure 32 - Software workflow

4.3. Mechanics architecture

The mechanics of the wearable device is as simple as a soft container with a spherical shape that enables the user to squeeze the ball without suffer any pain and protect the embedded electronics. In this project, an anti-stress ball is chosen to contain the whole system.

An anti-stress ball is a malleable object with a diameter not bigger than 7 cm, which is squeezed in the hand to relieve stress and muscle tension. There are different types of anti-stress ball depending on its building material:

- **Filled with gel**: these balls are made from a strong, durable rubber coating to ensure that the ball will not break with the repeated squeezing and stretching that comes with normal usage (Figure 33). Also, this coating prevents any leaks of the gel.
- **Filled with sand**: these balls are built using balloons which are filled with sand, rice (Figure 34), baking soda, etc. These materials have the malleable properties that are best suited to provide a certain level of resistance.
- **Non-filled**: these balls are made of a special malleable foam called closed-cell polyutherane foam rubber (Figure 35). The manufacturer injects a special liquid into a mould, resulting in a chemical reaction that creates carbon dioxide bubbles. These bubbles create the foam, which the mould forms into a soft shape.

Figure 33 - Anti-stress ball made of gel

Figure 34 - Anti-stress ball made of rice

Figure 35 - Anti-stress ball made of foam

The type of anti-stress ball that best suits the wearable device under design is the later one because the foam is solid enough to support the embedded electronics. Also, it allows an easier manipulation.

5. Wearable device: fast prototype design

The purpose of this section is to present the fast prototype design of the wearable device to fulfil the requirements listed in Table 13Table 7.

Table 13 - Requirements of the fast prototype design

#	Description of the requirement
13	Fast prototype design of the wearable device:
14	– as a proof-of-concept of the conceptual design.
15	– able to reliable measure some of Fried's frailty criteria.
16	– that can be used by an adult without the supervision of a doctor or a professional.
17	– with the lowest cost possible.
18	– with a friendly user interface.
19	– with a debugging interface for development phase.
20	– with a modular and scalable software architecture.

The whole system is embedded in a regular anti-stress ball with a size that enables both the integration of all the electronics and eases its manipulation. The wearable device is aimed to be able to measure the following frailty indicators:

- Grip strength (Fried's indicator)
- Sit-to-stand time (alternative indicator)
- Stand-to-sit time (alternative indicator)
- Walk time (Fried's indicator)

The user switches between measurement modes by pressing the ball and once the desired mode is selected, the wearable device starts measuring. The system finishes the current measurement, and transitions to standby mode, when the anti-stress ball is shaken. This basic operation totally matches with the target users, who tend to be old persons reluctant of complicated user interfaces.

The wearable device can be in six different modes that are explained in Table 14.

Table 14 - Modes of operation: fast prototype design

Mode	Description of mode
Standby	In this mode, the wearable device is in idle mode because there is no battery charge that needs to be saved.

Grip strength	In this mode, the wearable device starts measuring the pressure applied to the anti-stress ball for 5 seconds and stores the highest value of the grip strength into the non-volatile memory. Figure 15 shows a representation of this mode: when the mode is selected by pressing the anti-stress ball (step 1), the system starts acquiring the force applied (step 2); after 5 seconds, the user must shake the wearable device to return to standby (step 3).
Sit-to-stand	In this mode, the wearable device measures the time it takes to the user to go from a sitting position to a standing position and stores it into the non-volatile memory. Figure 16 shows a representation of this mode: when the mode is selected by pressing the anti-stress ball in a sitting position (step 1), the system starts a timer that stops when the user is in a standing position and shakes the wearable device (step 2); consequently, the system returns to standby.
Stand-to-sit	In this mode, the wearable device measures the time it takes to the user to go from a standing position to a sitting position and stores it into the non-volatile memory. Figure 17 shows a representation of this mode: when the mode is selected by pressing the anti-stress ball in a standing position (step 1), the system starts a timer that stops when the user is in a sitting position and shakes the wearable device (step 2); consequently, the system returns to standby.
Walk time	In this mode, the wearable device measures the time it takes to the user to travel a 4.5-meter distance and stores it into the non-volatile memory. Figure 18 shows a representation of this mode: when the mode is selected by pressing the anti-stress ball in a standing position (step 1), the system starts a timer that stops when the user has walked 4.5 meters and shakes the wearable device (step 2); consequently, the system returns to standby.
Data synchronization	In this mode, the wearable device transmits the data stored in the current session to the PC over the serial/debug communication link. Once this mode is selected and the data is correctly synchronized, the user must shake the wearable device to return to standby.

5.1. Hardware architecture

The measurement of the grip strength is based on a Force-Sensitive Resistor (FSR) and the measurement of movement, on an accelerometer. The output of these sensors is going to be processed by a microcontroller unit (MCU), which temporally stores the extracted information in RAM memory.

A wired serial UART communication is used to debug the system behaviour.

The MCU is also in charge of interfacing with the patient by means of an RGB LED, which will indicate the user in which state of operation is the wearable device.

Finally, the whole system is powered through a USB connection to the PC. The block diagram of the fast prototype wearable device is shown in Figure 36.

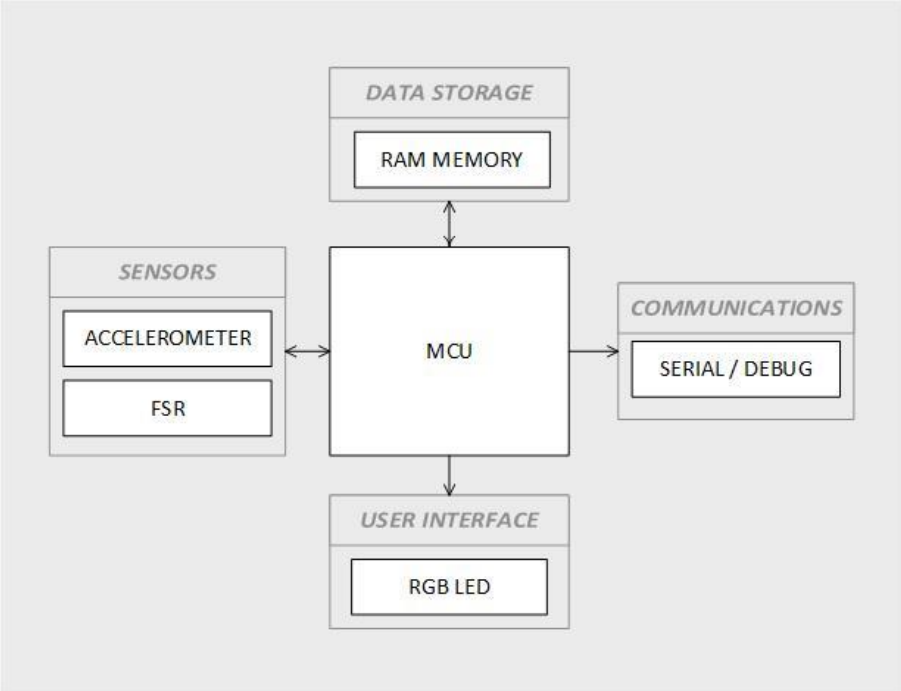

Figure 36 - System block diagram: fast prototype

5.1.1. Microcontroller unit

The microcontroller unit for the fast prototype is Microchip's PIC24FJ128GA204 because it is included in PIC24F Curiosity development board (Figure 37), a cost-effective development platform intended for those cases in which a feature-rich rapid prototyping board is required.

The development board is powered through a micro-B USB connector to supply 3.3 V to the PIC24FJ128GA204 and the whole system. The board integrates the PICkit On-Board (PKOB) circuit for basic programming and debugging.

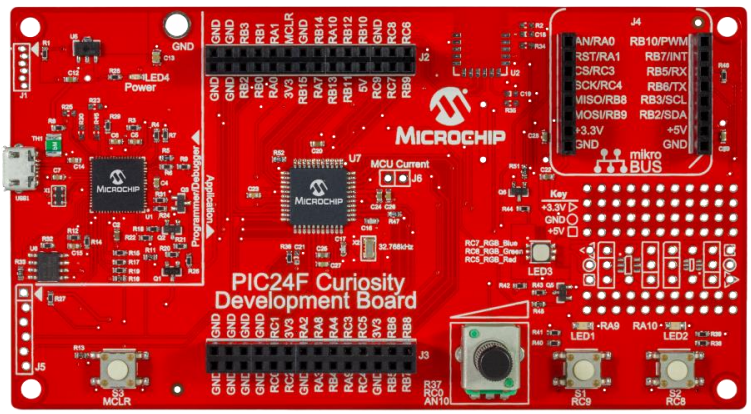

Figure 37 - PIC24F Curiosity development board

5.1.2. Sensors

5.1.2.1. Force-Sensing Resistor

There are no changes regarding the FSR block from conceptual design to fast prototype design.

5.1.2.2. Accelerometer

For the accelerometer MMA7455 sensor, the VM204 board (Figure 38) by Velleman is chosen because it includes the MMA7455 sensor and the appropriate conditioning circuitry. Additionally, it is a widely-used and low-cost accelerometer board for Arduino projects.

Figure 38 - Velleman's VM204 accelerometer board

5.1.3. Communications

5.1.3.1. Serial / Debug

For the fast prototype, the board in charge of changing from UART to USB standard is the BTE13-007 by BAITE (Figure 39).

Figure 39 - BAITE's BTE13-007 USB-to-UART board

5.1.4. User interface

There are no changes regarding the user interface block from conceptual design to fast prototype design.

5.1.5. Data storage

In the case of the fast prototype, the measurement obtained in a session are temporally stored in the RAM memory area of the PIC24FJ128GA204. Once the system is powered down, all the data is lost.

5.2. Software architecture

The fast prototype shall follow the modular and scalable software architecture of the wearable device. This means that the design will be able to support the addition of future features without incurring in higher costs in terms of development and integration. Figure 40 presents the software architecture of the system.

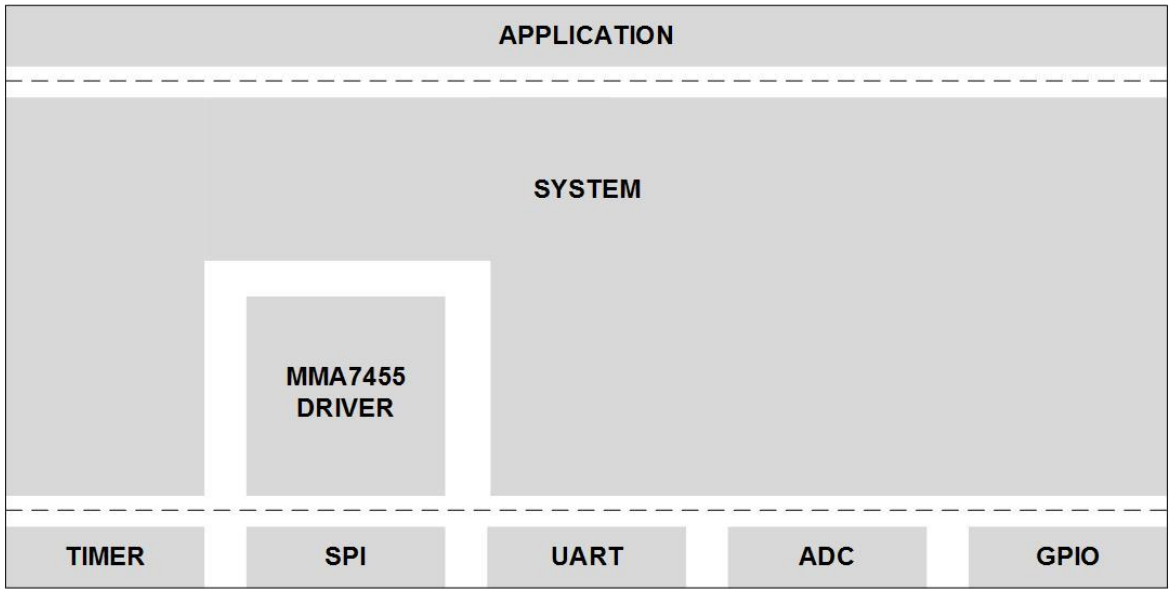

Figure 40 - Software architecture: conceptual design

The meaning of each of the modules in the software architecture is explained in Table 15.

Table 15 - Software modules description

Module	Description of the module
Application	The Application module handles the high-level operation of the wearable device such as state transitions.
System	The System module is the brain of the system since it configures all the peripherals of the MCU and acts as an interface between the Application and the drivers of the MMA7455.
MMA7455 Driver	The MMA7455 Driver handles the configuration and correct operation of the external MMA7455 chip.
Timer	The Timer module is used by the system to perform delays during the execution of the system.
SPI	The SPI module is used by the MMA7455 Driver to physically interface with the external chip.

UART	The UART module is used by the system to physically interface with the PC.
ADC	The ADC module is used by the system to sample the state of the input analogue channels such as the output voltage of the FSR's conditioning circuit.
GPIO	The GPIO module is used by the system to interact with the RGB LED.

The workflow of the embedded software is detailed in the diagram of Figure 32.

5.3. Mechanics architecture

Since the fast prototype design is based on a MCU included in a development board, the integration of the whole wearable device inside the anti-stress ball is discarded. However, it is still required to embed the FSR and accelerometer sensors as well as the user interface within the anti-stress ball. This means that there will be cables coming out from the anti-stress ball to the PIC24F development board.

6. Wearable device: fast prototype implementation

The purpose of this section is to present the fast prototype implementation of the wearable device to fulfil the requirements listed in Table 16.

Table 16 - Requirements of the fast prototype implementation

#	Description of the requirement
21	Implementation of the wearable device fast prototype:
22	– following the system software architecture.
23	– made of off-the-shelf electronic components.
24	– with the electronic system embedded in the mechanic system.
25	– enables an easy real testing of the system.

6.1. Hardware implementation

6.1.1. MCU interface

The PIC24F Curiosity development board includes two 2x14 female headers (J2 and J3) that enables the connectivity of PIC24FJ128GA204 to the outer world. These two headers are used by the fast prototype to connect the embedded electronics inside the anti-stress ball and the MCU. Table 17 shows the wired connection between the development board and the anti-stress ball.

Table 17 - MCU pin mapping

Header	Pin	Meaning	Wire colour	Destination in the anti-stress ball
J3	18	3V3	Red	Power supply line.
J3	22,24,26,28	GND	Orange	Ground reference.
J3	16	RA2	Yellow	Green pin of the RGB.
J3	8	RC5	Green	Blue pin of the RGB.
J3	4	RB6	Blue	Red pin of the RGB.
J2	23	RB2	Purple	Voltage output of the FSR sensor conditioning circuit.
J2	1	RB9	Grey	Chip select (active low) of the VM204 accelerometer sensor SPI interface.
J2	3	RC7	White	Master-In-Slave-Out of the VM204

				accelerometer sensor SPI interface.
J2	15	RB15	Black	Master-Out-Slave-In of the VM204 accelerometer sensor SPI interface.
J2	21	RB0	Brown	Serial Clock of the VM204 accelerometer sensor SPI interface.

6.1.2. Embedded electronics

This section describes the embedded electronics into the anti-stress ball.

6.1.2.1. Force Sensing Resistor

The output voltage of the FSR conditioning circuit is obtained with the following relationship:

$$V_{OUT} = V_{REF} \cdot \left(1 + \frac{R_F}{R_{FSR}}\right)$$

The voltage reference has been implemented with a simple voltage divider consisting on a pull-up resistor of 10 kΩ and a pull-down resistor of 2.2 kΩ, which gives a voltage reference of 0.595 V. The voltage reference is the voltage that the block will present when no force is applied to the FSR; therefore, it is required to be low enough to have a large dynamic range. The minimum resistance experimentally captured of the FSR around 400 Ω. Once the voltage reference and the minimum resistance of the FSR are known, there is only missing the feedback resistor (R_F). The choice of the feedback resistor is based on the V_{OUT} vs. FSR Resistance characteristic shown in Figure 41. The curve that has the largest dynamic range without surpassing the 3.3 V of the power supply is for a feedback resistor of 1 kΩ.

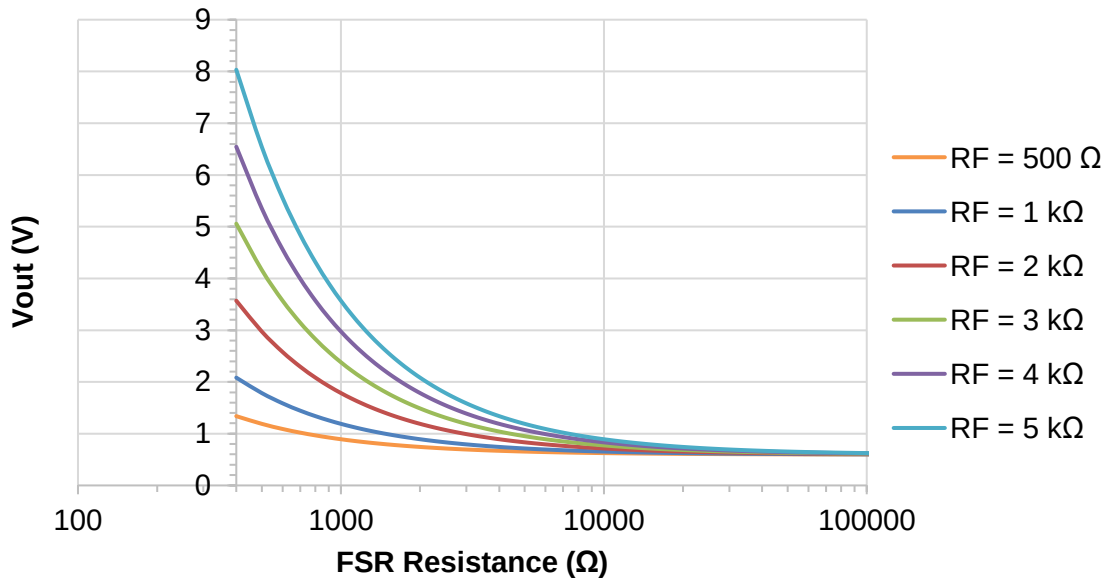

Figure 41 - V_{OUT} (V) vs. FSR Resistance (Ω) characteristic

6.1.2.2. Accelerometer

The VM204 accelerometer sensor board is totally integrated into the board that resides in the anti-stress ball. The four SPI wires are connected to the MCU interface as wells as the 3.3V and GND power lines.

The MMA7455 is configured via an SPI connection where the MCU acts as the master and the accelerometer, as the slave. The MCU drives the clock (SCLK), the Chip Select (CSn) and the Master-Out Slave-In (MOSI) signals; whereas the slave, the accelerometer, only drives the Master-In Slave-Out signal (MISO). As depicted in Figure 42, every data transfer in the SPI interface lasts 16 clock cycles, in which the Chip Select signal shall be driven low because it is low-active. The clock signal is at low level when idle and coordinates the sampling and shifting of data: data is sampled at rising edges and shifted at falling edges.

The first 8-bits are always sent by the master. The first bit informs the slave whether the command is for reading (0) or writing (1) and the next 6 bits indicate the targeted register. The eight bit is ignored. The following 8 bits are either the data of the requested register (read operation) or the data to be written in the register (write operation).

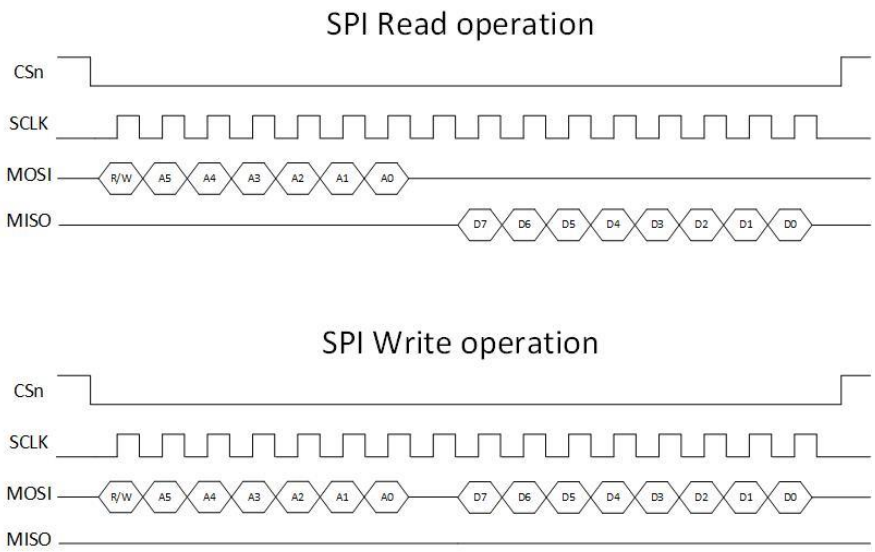

Figure 42 - SPI data transfer

6.1.2.3. RGB LED

The RGB LED chosen for the implementation of the fast prototype presents a common cathode. It has not been possible to find the reference of the RGB LED (Figure 43), therefore, the choice of the 100-Ω limiting current resistor placed on the common cathode has been based on an iterative manual testing to maximize its brightness.

Figure 43 - RGB LED pin diagram

The following table shows the pin mapping of the RGB LED used in the fast prototype.

Table 18 - RGB LED pin mapping

Pin number	Pin meaning
1	Red
2	Common cathode
3	Blue
4	Green

6.1.3. Serial/Debug communication

The UART transmission stream is output at RC0 (pin 19 of J3 of PIC24F Curiosity development board) from the MCU and received at RXD line of BTE13-007 USB-to-UART board, which is connected to the PC (Figure 44).

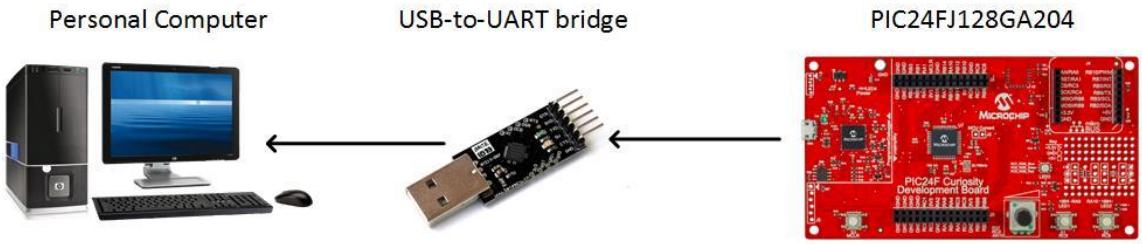

Figure 44 - Serial/Debug communication implementation

The baud rate of the UART communication is set to 9600 bps with no parity bit and one single stop bit. To read the output stream of the MCU, it is required a serial console in the personal computer. In this project, PuTTY application is used because it is free and open-source.

6.2. Software implementation

The software modules and the correspondent source and header files are listed in Table 19.

Table 19 - Software modules: source and header files

Module	Source File	Source Header
Application	main.c	-
System	system.c	system.h
MMA7455 Driver	mma7455.c	mma7455.h
Timer	timer.c	timer.h
SPI	spi.c	spi.h
UART	uart.c	uart.h
ADC	adc.c	adc.h
GPIO	led.c	led.h

6.2.1. Application

The main routine of main.c source file calls the system initialization and starts the while-loop that implements the state-machine of the wearable device. The mode transitions and calls to different types of measurements are done in the while-loop.

6.2.2. System

The methods implemented in system.c source file are listed in Table 20.

Table 20 - Methods in system.c

Method name	Method description
void system_Init(void)	This method wraps all internal initialization calls.
void system_pinInit(void)	This method configures the output and input pins of the MCU.
void system_comInit(void)	This method initializes the UART, SPI and GPIO peripherals.
void system_adcInit(void)	This method configures the ADC module.
void system_mma7455Init(void)	This method resets and calibrates the MMA7455 accelerometer sensor.
unsigned char system_getSystemMode(void)	This method returns the current system mode.
void system_setSystemMode(	This method sets the next system mode.

unsigned char nextSystemMode)	
void system_storeDataElement(system_dataElement_t dataElement)	This method stores a new measurement into memory.
void system_gripStrength(void)	This method performs the grip strength measurement.
void system_sit2Stand(void)	This method performs the sit-to-stand measurement.
void system_stand2Sit(void)	This method performs the stand-to-sit measurement.
void system_walkTime(void)	This method performs the walk time measurement.
void system_syncData(void)	This method output all the acquired results over the serial/debug communication link.
unsigned int system_counts2time(unsigned int counts)	This method transform timer counts to time in milliseconds.
void system_printLogo(void)	This method prints the logo of the wearable device.

6.2.3. MMA7455 driver

The methods implemented in mma7455.c source file are listed in Table 21Table 22.

Table 21 - Methods in mma7455.c

Method name	Method description
void mma7455_reset(void)	This method resets the MMA7455 registers.
void mma7455_calibration(void)	This method performs the required initial calibration to obtain proper acceleration measurements.
void mma7455_setupMeasurementMode(void)	This method sets the MMA7455 in measurement mode.
void mma7455_waitFreefall(void)	This method is blocking until a freefall is detected in any axis.
void mma7455_printRegisters(void)	This method prints the value of all MMA7455 registers.
void mma7455_printAxisStatus(void)	This method prints the current acceleration of

	all three axis.
char mma7455_getXAxisAcceleration(void)	This method reads the current acceleration in X axis.
char mma7455_getYAxisAcceleration(void)	This method reads the current acceleration in Y axis.
char mma7455_getZAxisAcceleration(void)	This method reads the current acceleration in Z axis.

6.2.4. Timer

The methods implemented in timer.c source file are listed in Table 22.

Table 22 - Methods in timer.c

Method name	Method description
void timer1_start(unsigned char mode)	This method starts a 0.5-second timer for the blinking RGB LED. Indirectly, the same timer is counting 5 seconds.
void timer1_stop(void)	This method stops the timer for the blinking RGB LED.
void timer3_start(void)	This method starts the timer used to measure the time of sit-to-stand, stand-to-sit and walk modes.
unsigned int timer3_stop(void)	This method stops the timer used to measure the time of sit-to-stand, stand-to-sit and walk modes and returns the number of counter clock ticks.
void timer2_wait(unsigned int ms)	This method is used to perform delays.
void __attribute__((__interrupt__,auto_psv)) _T1Interrupt(void)	This interrupt service routine is used to handle the blinking RGB LED and the 5-second timeout.

6.2.5. SPI

The methods implemented in spi.c source file are listed in Table 23.

Table 23 - Methods in spi.c

Method name	Method description
void spi1_config(void)	This method configures SPI1 module as

	master in mode 0 with 16-bit data exchange at a baudrate of 50 kbps.
unsigned int spi1_readRegister(**unsigned char registerAddress)**	This method accesses the 8-bit data contents of a register via its 6-bit address.
void spi1_writeRegister(**unsigned char registerAddress,** **unsigned char registerValue)**	This method writes 8 bits of data into a register via its 6-bit address.

6.2.6. UART

The methods implemented in uart.c source file are listed in Table 24.

Table 24 - Methods in uart.c

Method name	Method description
void uart1_config(void)	This method configures UART1 module with 8-bit data transfer, 1 stop-bit, no parity and a baud rate of 9600 bps.

6.2.7. ADC

The methods implemented in adc.c source file are listed in Table 25Table 24.

Table 25 - Methods in adc.c

Method name	Method description
void adc_config(void)	This method configures the 10-bit ADC module with 3.3 V as positive voltage reference, ground as negative voltage reference and the data result as absolute unsigned value.
unsigned short adc_read(void)	This method reads the current sampled value by the ADC module.

6.2.8. GPIO

The methods implemented in led.c source file are listed in Table 26.

Table 26 - Methods in led.c

Method name	Method description
void led_config(void)	This method initializes the RGB LED GPIO lines.

void led_setColour(unsigned char colour)	This method sets the RGB LED GPIO lines according to a given colour code.
void led_toggle(unsigned char ledState)	This method toggles the RGB LED GPIO lines resulting in the blinking RGB LED behaviour.

6.3. Mechanics implementation

During the development of the project there have been two anti-stress alternatives: a 6-cm diameter ball (Figure 45) and a 7-cm diameter ball (Figure 46).

Figure 45 - 6-cm diameter blue anti-stress ball

Figure 46 - 7-cm diameter multicolour anti-stress ball

The 6-cm diameter ball has been finally discarded because it is too small to fit the size of the implemented PCB. Also, as shown in Figure 47 and Figure 48 the resistance to compression force of the blue anti-stress ball is lower than for the multicolour one.

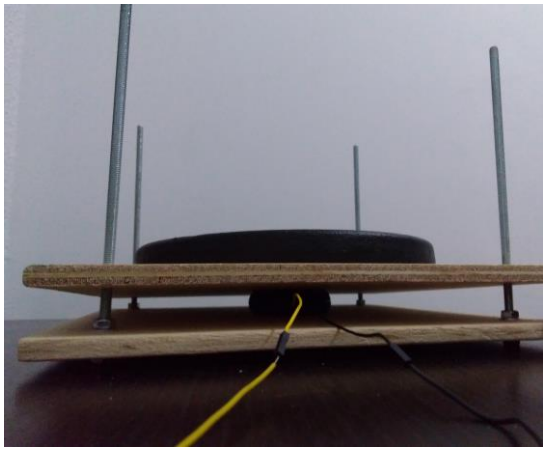

Figure 47 - Blue ball in deadweight measurement system (5 kgf)

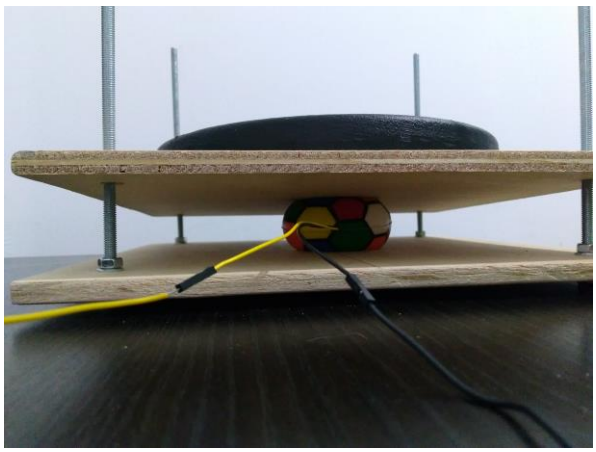

Figure 48 - Multicolour ball in deadweight measurement system (5 kgf)

7. Deadweight measurement device

The FSR sensor shall be first calibrated to obtain the force to resistance characteristic. Unfortunately, there was no availability of a compressive force measurement device that could have been used to calibrate the anti-stress ball. Therefore, it has been required to design and implement an ad-hoc system to be able to calibrate the FSR sensor. This compressive force measurement system is based on the deadweight principle. The requirements of the deadweight measurement device are shown in the table below.

Table 27 - Project requirements from deviations

#	Description of the requirement
26	Design of a deadweight measurement device able to reliable measure a compression force.
27	Implementation of a deadweight measurement device able to reliable measure a compression force.

As shown in Figure 49, the grip ball is placed between two wooden boards. The top board is where the weight plates of known mass are placed. This way, the force of the mass of the weight plates is applied to the grip ball. Both wooden boards are attached to each other via four metallic rods.

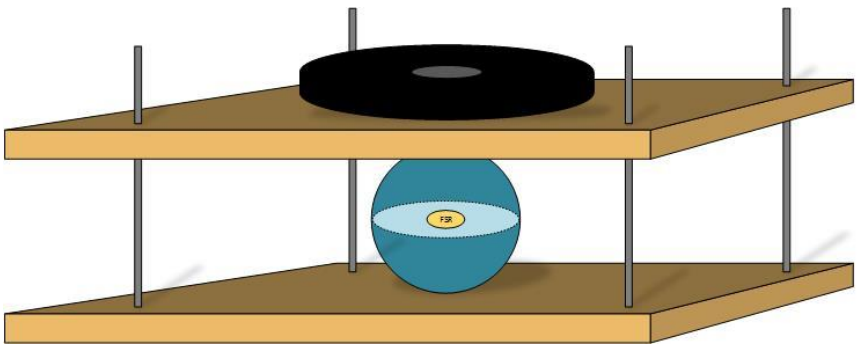

Figure 49 - Deadweight measurement system: diagram

Below, some pictures of the real deadweight measurement system are shown.

Figure 50 - Deadweight measurement system: bottom wooden board

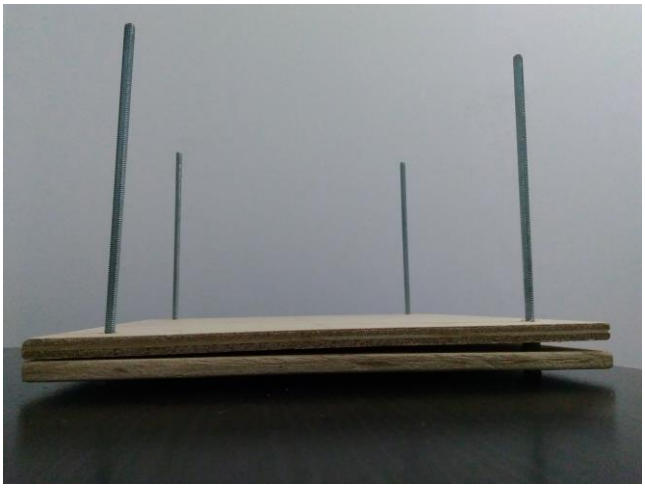

Figure 51 - Deadweight measurement system: both wooden boards

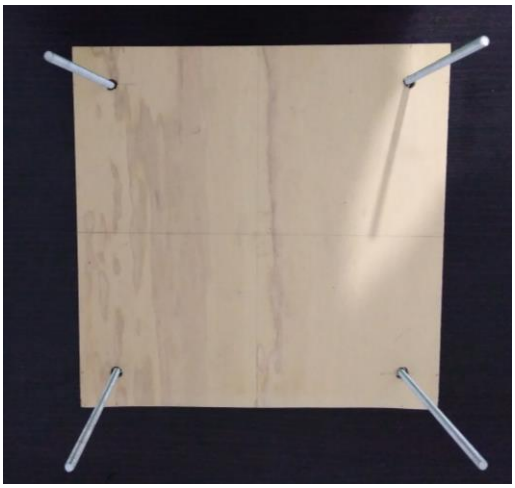

Figure 52 - Deadweight measurement system: top view

The calibration range goes from 1 Kilogram-force (kgf) to 40 kgf. To achieve so, the following set of weight plates has been used.

Table 28 - Weight plate configuration for 1-10 kgf

Weight plate	Kilograms-force applied									
	1	2	3	4	5	6	7	8	9	10
1 kg	1	-	1	-	-	1	-	1	-	-
2 kg	-	1	1	2	-	-	1	1	2	-
5 kg	-	-	-	-	1	1	1	1	1	2

Table 29 - Weight plate configuration for 11-20 kgf

Weight plate	Kilograms-force applied									
	11	12	13	14	15	16	17	18	19	20

1 kg	1	-	1	-	-	1	-	1	-	-
2 kg	-	1	1	2	-	-	1	1	2	-
5 kg	2	2	2	2	3	3	3	3	3	4

Table 30 - Weight plate configuration for 21-30 kgf

Weight plate	**Kilograms-force applied**									
	21	22	23	24	25	26	27	28	29	30
1 kg	1	-	1	-	1	-	1	-	1	-
2 kg	-	1	1	2	2	3	3	4	4	5
5 kg	4	4	4	4	4	4	4	4	4	4

Table 31 - Weight plate configuration for 31-40 kgf

Weight plate	**Kilograms-force applied**									
	31	32	33	34	35	36	37	38	39	40
1 kg	1	-	1	2	3	4	5	6	7	8
2 kg	5	6	6	6	6	6	6	6	6	6
5 kg	4	4	4	4	4	4	4	4	4	4

8. Results

8.1. Conceptual design of the wearable device

The schematic of the conceptual design of the wearable device can be found in Annex A.

8.2. Fast prototype hardware

The implementation of the fast prototype is the major physical outcome of this project: going from the conceptual design of the wearable device to the real implementation of the fast prototype.

The result of the fast prototype implementation is divided into three different items: the embedded electronics, the MCU interface and the anti-stress ball modification.

8.2.1. Embedded electronics

The embedded electronics of the anti-stress ball include the FSR sensor and conditioning circuitry, the accelerometer sensor and the user interface. The embedded electronics has been stacked in three different layers: the lower one is where the electronics components are located, the middle one is for the VM204 accelerometer sensor board and the upper one serves as a solid support for the FSR.

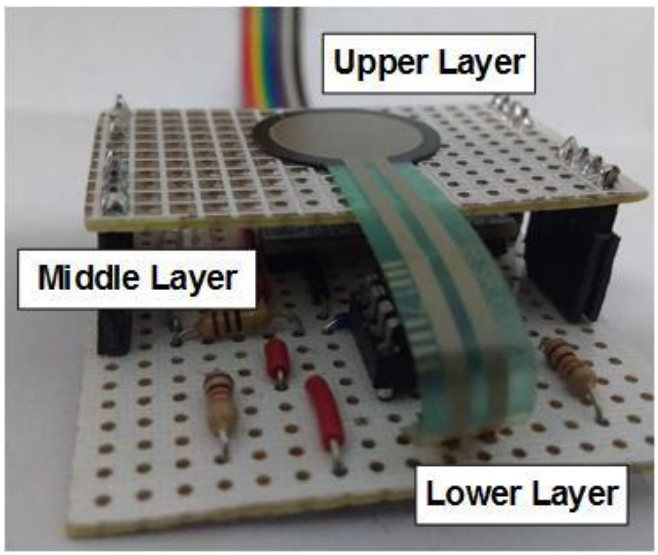

Figure 53 - Embedded electronics: layers

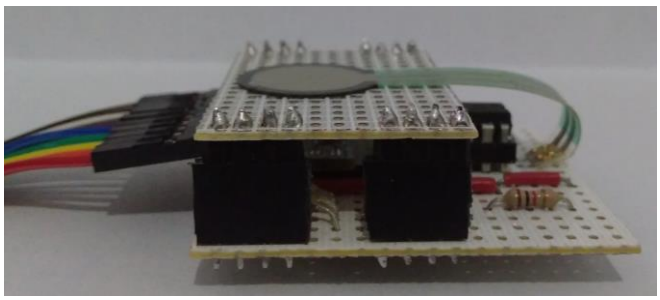

Figure 54 - Embedded electronics: side view

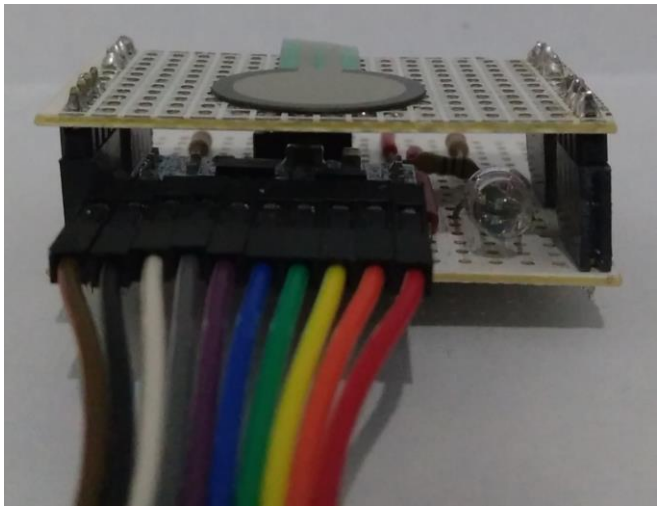

Figure 55 - Embedded electronics: front view

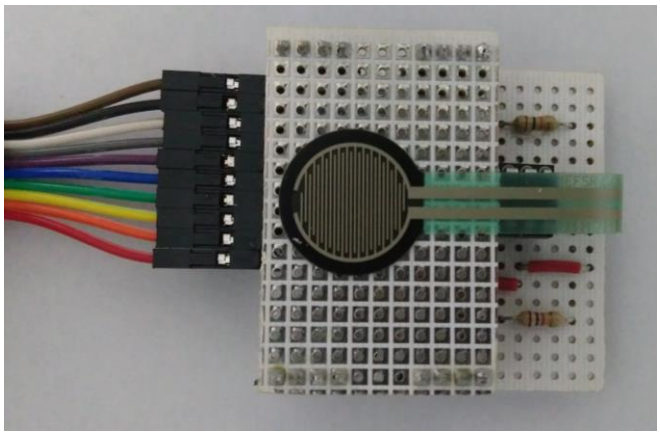

Figure 56 - Embedded electronics: top view

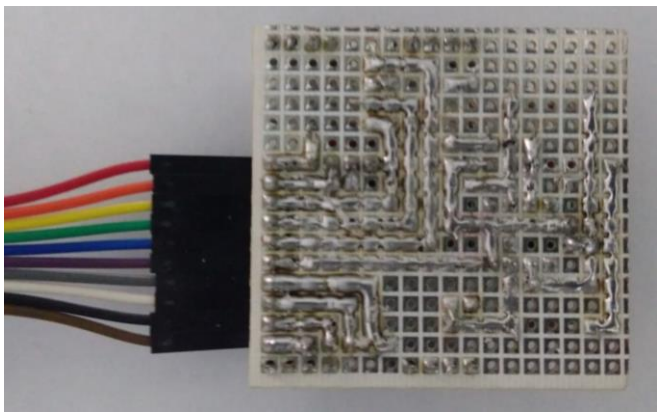

Figure 57 - Embedded electronics: bottom view

The schematic of the fast prototype hardware implementation can be found in Annex B.

8.2.2. I/O extension board

An ad-hoc PCB has been required to be implemented so as to easily connect the inputs and outputs of the embedded electronics to the PIC24F Curiosity development board. The Arduino philosophy of stacked extension boards has been followed.

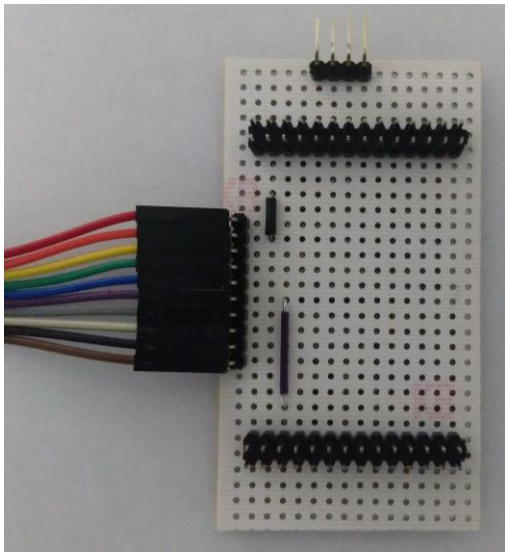

Figure 58 - I/O extension board: bottom view

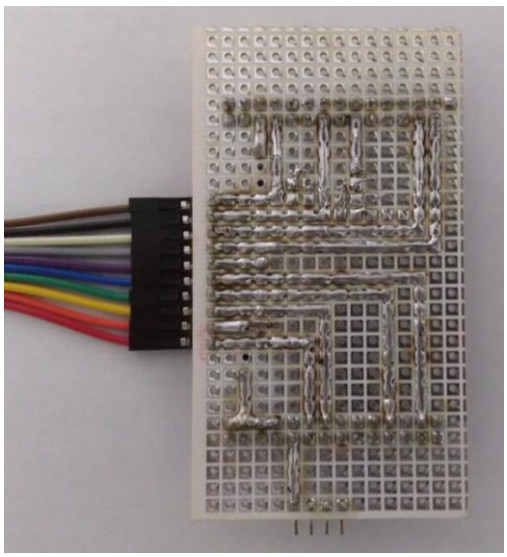

Figure 59 - I/O extension board: top view

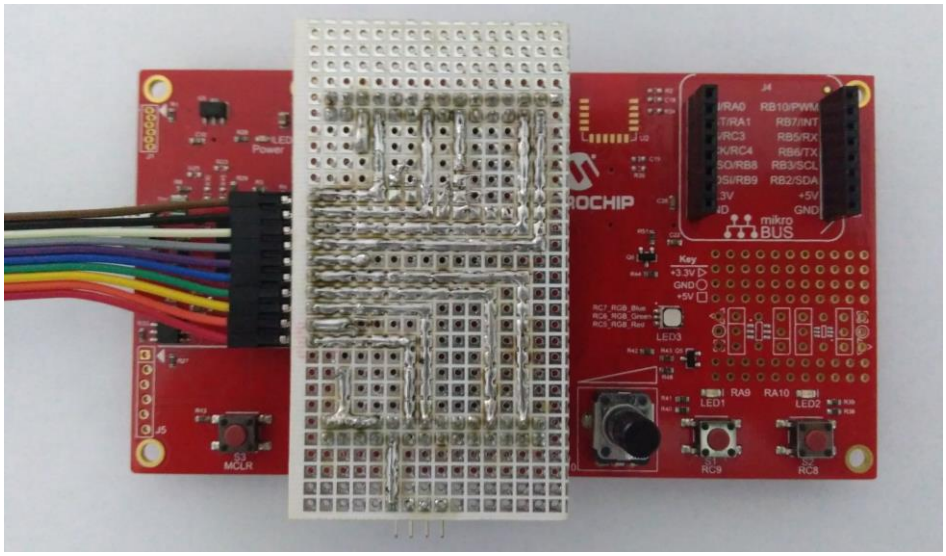

Figure 60 - I/O extension board on PIC24F Curiosity development board: top view

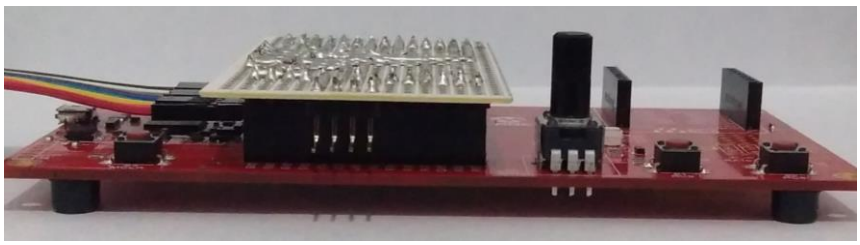

Figure 61 - I/O extension board on PIC24F Curiosity development board: side view

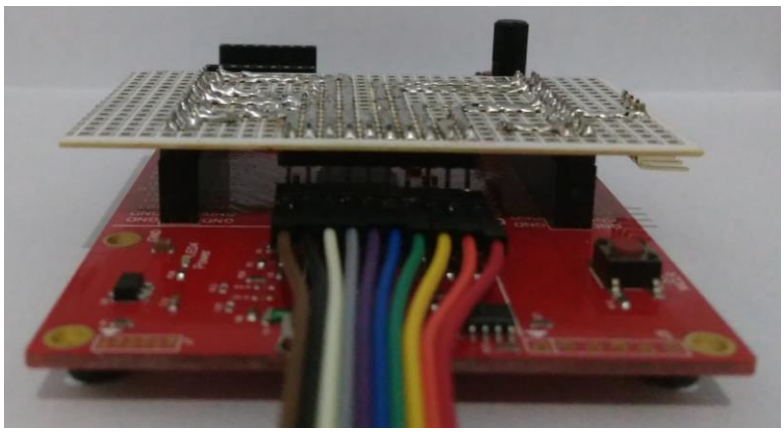

Figure 62 - I/O extension board on PIC24F Curiosity development board: front view

8.2.3. Anti-stress ball modification

The anti-stress ball has been modified to be able to host the embedded electronics in the most suitable way. To achieve so, the anti-stress ball has been split in two halves and the shape of the embedded electronics has been sculpt in each half.

Figure 63 - Original anti-stress ball

Figure 64 - Modified anti-stress ball

8.2.4. Integration

The integration of the embedded electronics into the anti-stress ball is shown in the figures below.

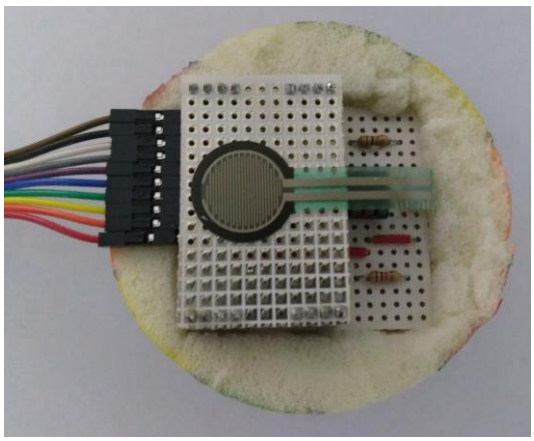

Figure 65 - Embedded electronics integrated into anti-stress ball

Figure 66 - Closed anti-stress ball

8.3. Fast prototype software

The software developed for the fast prototype is also an important deliverable of this project and thus the source files are included in Annex C.

8.4. FSR calibration with deadweight measurement system

The principal deviation from the initial plan was the inability to calibrate the FSR sensor embedded in the anti-stress ball due to the lack of a compressive measurement device in the laboratory premises. To overcome this show stopper, it was decided to build a custom deadweight measurement system for the calibration.

The calibration procedure is described in the following steps:

1. Deposit the set of weight plates on the top wooden board.
2. Use a level at the centre of the deadweight measurement system and at the top of the weight plates to equilibrate the top wooden board.
3. Acquire 20 samples of the output voltage from the FSR conditioning circuit with a delay of 0.5 seconds between them.
4. Compute the arithmetic mean.
5. Repeat from step 1.

An example of the setup for 40 kgf is shown in figure below.

Figure 67 - Calibration of the FSR: 40 kgf setup

The calibration range goes from 0 kgf to 40 kgf and the obtained characteristic of compressive force applied (kgf) vs. V_{OUT} (mV) is shown in Figure 68. The plot shows the real curve that maps the applied force to the output voltage and a linearization of this curve. The linearized curve has the following equation:

$$V_{OUT}\ (mV) = 26.221 \cdot Applied\ force\ (kgf) + 634.83$$

But, it is noticeable that the linearization does not fit for all the curve. For a better insight, Figure 69 shows the error introduced by the linearization for each applied force. At some points of the curve, the error even deviates 2.5 kgf from the real applied force.

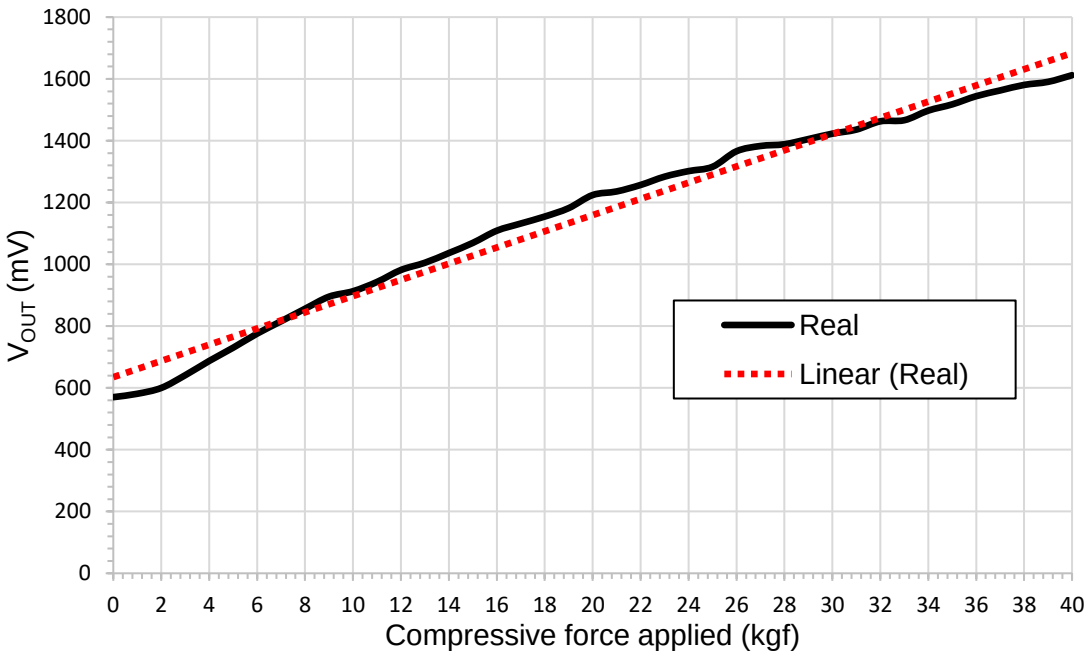

Figure 68 - Compressive force applied (kgf) vs. V_{OUT} (mV) characteristic

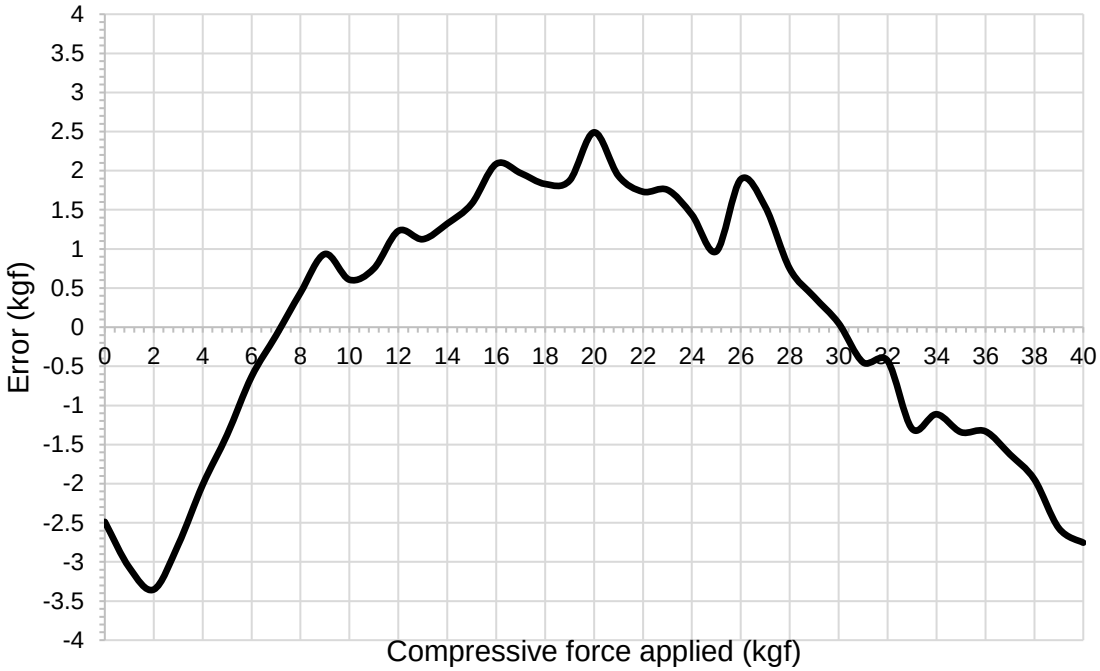

Figure 69 - Compressive force applied (kgf) vs. error (kgf) characteristic

One possible approach to linearize the characteristic is to split the curve into sections:

- The first section of the graph (from 0 kgf to 3 kgf) can be neglected since no change in output voltage is observed.
- The second section of the graph (from 4 kgf to 20 kgf) has a slightly different slope.
- The third section of the graph (from 21 kgf to 40 kgf) has a different slope as well.

With this division, the linearization of the second part is shown in Figure 70. The error introduced by the linearization is now reduced to less than 1 kgf (Figure 71). The linearized curve for the second section has the following equation:

$$V_{OUT}\ (mV) = 32.241 \cdot Applied\ force\ (kgf) + 584.22$$

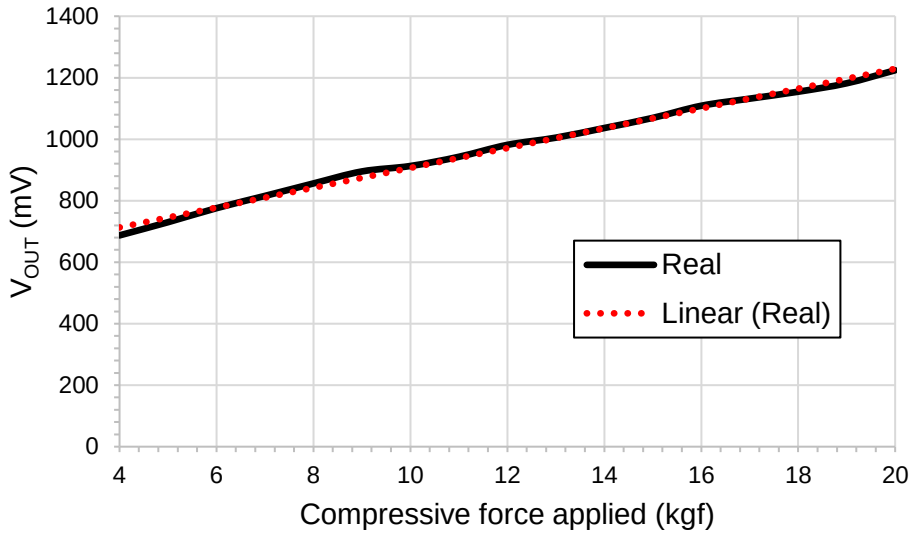

Figure 70 - Compressive force applied (kgf) vs. V_{OUT} (mV) characteristic: second section

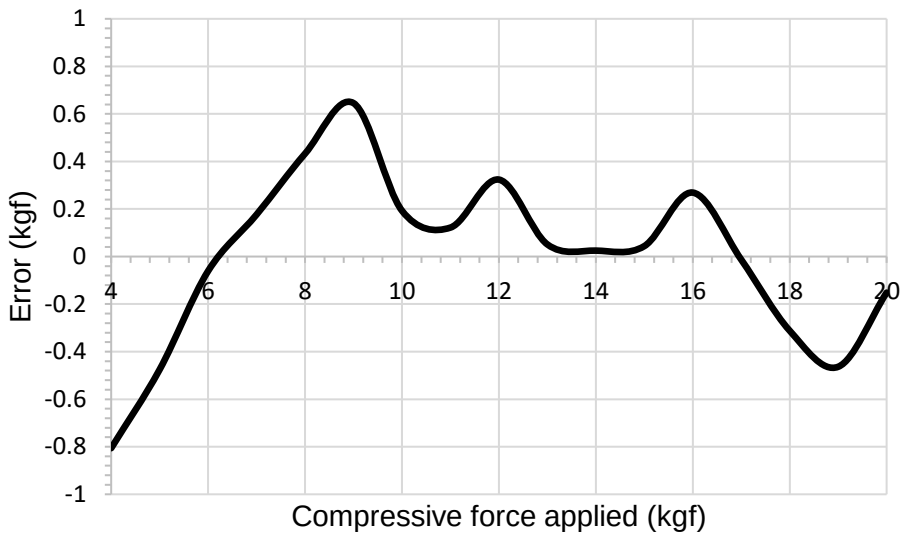

Figure 71 - Compressive force applied (kgf) vs. error (kgf) characteristic: second section

The linearization of the third part is shown in Figure 72Figure 70. The error introduced by the linearization is now reduced to less than 1 kgf (Figure 73), except from an spurious data at 27 kgf. The linearized curve for the second section has the following equation:

$$V_{OUT}\ (mV) = 19.489 \cdot Applied\ force\ (kgf) + 836.99$$

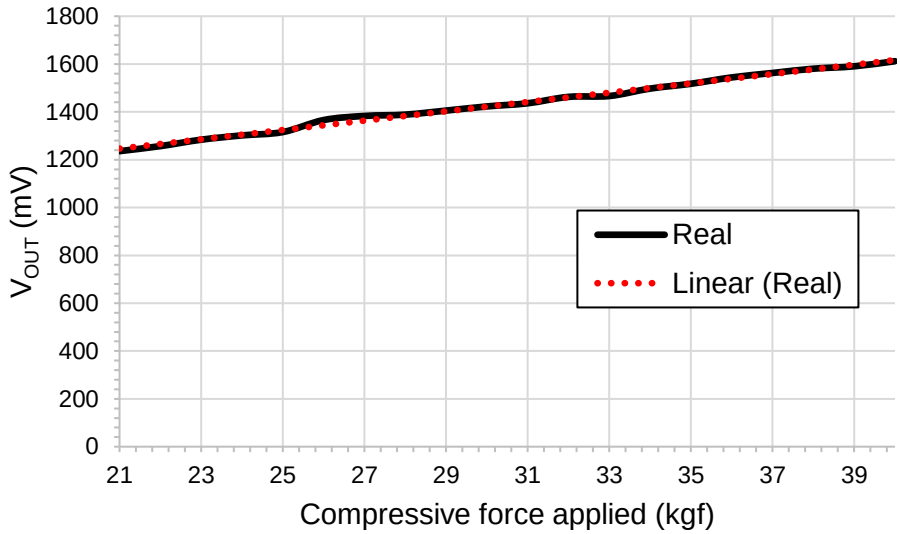

Figure 72 - Compressive force applied (kgf) vs. V_{OUT} (mV) characteristic: third section

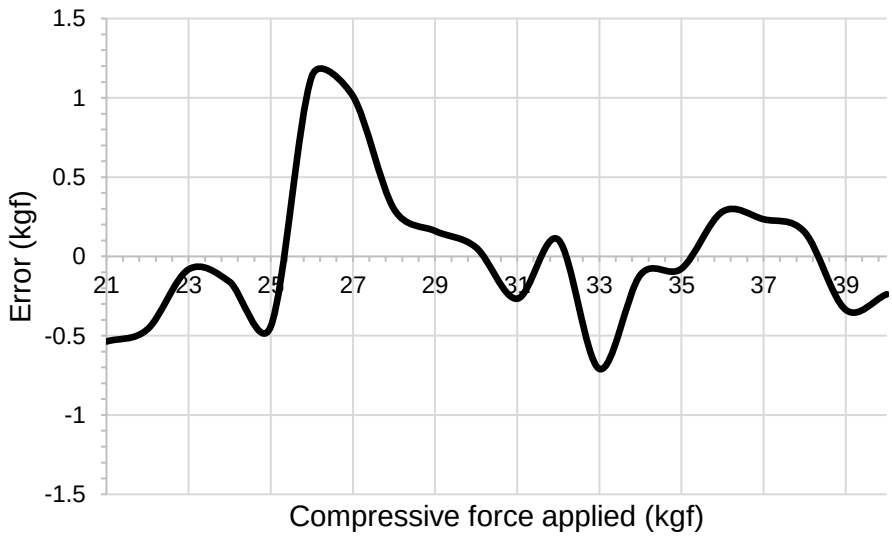

Figure 73 - Compressive force applied (kgf) vs. error (kgf) characteristic: third section

Once the original characteristic has been divided in three different sections, the wearable device needs the reciprocal function to obtain the compressive force applied from the acquired FSR system output voltage:

Table 32 - Applied force equations for wearable device

V_{OUT} range (mV)	Equation
$V_{OUT} < 713.184$	None
$713.184 \leq V_{OUT} \leq 1229.04$	$Applied\ force\ (kgf) = \frac{V_{OUT}(mV) - 584.22}{32.241}$
$V_{OUT} > 1229.04$	$Applied\ force\ (kgf) = \frac{V_{OUT}(mV) - 836.99}{19.489}$

9. Budget

The purpose of this chapter is to detail the overall costs of the project as well as the unitary cost of the implemented wearable device fast prototype. Since I already owned some of the tools and materials used in this project, the criteria to include them in the costs is the following: if the item is specifically needed for the development of the project, it will be considered in the costs. For instance, for software development and documentation, a personal computer is obviously needed; but, since any personal computer could have been used, the cost of the personal computer is omitted. The same happens with the soldering iron because there are not any specific requirements: any soldering iron could have been used.

The breakout of the costs comprehends the following categories:

- **Software**: required software tools for development and documentation.
- **Hardware**: electronic components either included in the fast prototype or used in any phase of the project.
- **Mechanics**: tools and objects used to develop the fast prototype.
- **Engineering Services**: hours dedicated to the project either by the author or the advisor.

9.1. Overall project costs

The overall project costs categorization includes all the items that have been purchased throughout the progress of the project. The table below summarizes the overall project costs.

Table 33 - Overall project costs by category

Category	Cost (€)
Software	0
Hardware	81,32
Mechanics	69,15
Engineering Services	1740,00
TOTAL	**1890,47**

The costs of each category are detailed in subsequent sections.

9.1.1. Software

Table 34 - Overall project costs in software

Item	Cost (€)
MPLAB X Integrated Development Environment	0
MPLAB XC16 Compiler	0
KiCad Electronics Design Automation Suite	0
PuTTY	0
GitHub Repository	0
TOTAL	**0**

9.1.2. Hardware

Table 35 - Overall project costs in hardware

Hardware	Unitary Cost (€)	Quantity	Cost (€)
Microchip PIC24F Curiosity Development Board	24,520	1	24,52
USB-to-UART TTL CP2102 Module	5,900	1	5,90
Interlink Electronics FSR 402	5,950	2	11,90
Interlink Electronics FSR 406	7,030	2	14,06
Velleman 3-Axis Digital Accelerometer Sensor Module VM204	5,050	1	5,05
4-pin RGB LED	0,940	2	1,88
MCP6273 Operational Amplifier	0,490	1	0,49
100 Ohms Resistor	0,350	1	0,35
1000 Ohms Resistor	0,100	1	0,10
2200 Ohms Resistor	0,150	1	0,15
10000 Ohms Resistor	0,100	1	0,10
Repro 77x90mm Baquelita PCB	3,190	1	3,19
8-pin Socket	0,255	4	1,02
Straight Male Header	0,022	40	0,88
Right-Angle Male Header	0,029	40	1,16
Straight Double Male Header	0,018	40	0,72
Straight Female Header	0,037	36	1,33
30-cm Female-Male Flat Cables	0,113	40	4,52
30-cm Female-Female Flat Cables	0,100	40	4,00
TOTAL			**81,32**

9.1.3. Mechanics

Table 36 - Overall project costs in mechanics

Mechanics	Unitary Cost (€)	Quantity	Cost (€)
7-cm diameter multicolour ball	0,99	2	1,98
6-cm diameter blue ball	0,98	1	0,98
600x300x10mm Plywood	4,09	1	4,09
20cm Rod + Female Screw x 4	1,55	4	6,20
5-kg Plate x 4	6,45	4	25,80
2-kg Plate x 6	2,95	6	17,70
1-kg Plate x 8	1,55	8	12,40
TOTAL			**69,15**

9.1.4. Engineering Services

Table 37 - Overall project costs in engineering services

Engineering Services	Cost/hour (€)	Hours/week	Weeks of work	Cost (€)
Engineer	10	5	30	1500
Advisor	16	0,5	30	240
TOTAL				**1740,00**

9.2. Unitary cost of fast prototype

The unitary cost of the fast prototype includes all the items that have been purchased and used to build it. The table below summarizes the unitary cost of the fast prototype.

Table 38 - Unitary cost of fast prototype by category

Category	Cost (€)
Software	0
Hardware	54,76
Mechanics	0,99
Engineering Services	108,00
TOTAL	**163,75**

The costs of each category are detailed in subsequent sections.

9.2.1. Software

Table 39 - Unitary cost of fast prototype in software

Item	Cost (€)
MPLAB X Integrated Development Environment	0
MPLAB XC16 Compiler	0
KiCad Electronics Design Automation Suite	0
PuTTY	0
GitHub Repository	0
TOTAL	**0**

9.2.2. Hardware

Table 40 - Unitary cost of fast prototype in hardware

Hardware	Unitary Cost (€)	Quantity	Cost (€)
Microchip PIC24F Curiosity Development Board	24,520	1	24,52
USB-to-UART TTL CP2102 Module	5,900	1	5,90
Interlink Electronics FSR 402	5,950	1	5,95
Velleman 3-Axis Digital Accelerometer Sensor Module VM204	5,050	1	5,05
4-pin RGB LED	0,940	1	0,94
MCP6273 Operational Amplifier	0,490	1	0,49
100 Ohms Resistor	0,350	1	0,35
1000 Ohms Resistor	0,100	1	0,10
2200 Ohms Resistor	0,150	1	0,15

10000 Ohms Resistor	0,100	1	0,10
Repro 77x90mm Baquelita PCB	3,190	1	3,19
8-pin Socket	0,255	1	0,26
Straight Male Header	0,022	16	0,35
Right-Angle Male Header	0,029	24	0,70
Straight Double Male Header	0,018	28	0,50
Straight Female Header	0,037	16	0,59
30-cm Female-Male Flat Cables	0,113	40	4,52
30-cm Female-Female Flat Cables	0,100	11	1,10
TOTAL			**54,76**

9.2.3. Mechanics

Table 41 - Unitary cost of fast prototype in mechanics

Mechanics	Unitary Cost (€)	Quantity	Cost (€)
7-cm diameter multicolour ball	0,99	1	0,99
TOTAL			**0,99**

9.2.4. Engineering Services

Table 42 - Unitary cost of fast prototype in engineering services

Engineering Services	Cost/hour (€)	Hours/week	Weeks of work	Cost (€)
Engineer	10	5	2	100
Advisor	16	0,5	1	8
TOTAL				**108,00**

10. Conclusions and future development

Frailty in elder people is becoming a major concern with the passage of years because of the world population ageing. This phenomenon is based on the reduction of fertility rates and the rising of life expectancy. For the later, the main reasons of having a global average life expectancy of 71.4 years - according to World Health Organization - are the progress in diagnosis technologies, the continuous investigation in treatments and the worldwide interest in healthy habits.

In this new humankind era, the early diagnosis of frailty might be used to prevent and care in a better manner the health of a person, and thus, improve his/her life conditions. Is, in this philosophy, where the development of this project has been focused at.

The goals of this project were the design of a wearable device to measure some of the Fried's frailty indicators, design and implement a fast prototype of the wearable device and design and implement a compressive force calibration system. Once the project has finished, a proper way to evaluate the results is to check whether the requirements stated in the introduction of this document have been finally fulfilled or not.

The concept of the wearable device is designed to measure grip strength and walk time - both are part of Fried's frailty criteria - in a reliable basis. Additionally, the wearable device has a low energy consumption by design, allowing this way the integration of an small battery. The system has a user-friendly interface due to its press-and-shake operation along with a RGB LED indicator, which also enables the usage of the wearable device without the supervision of a professional. However, the press-and-shake concept shall be tested on old adults with Parkinson, for instance, because it could lead to wrong results and bad user experience. A wireless communication as wells as a serial debug interface have been enabled in the design. But, one of the major drawbacks has been the lack of a design for the wireless power transfer charging system. The choice of components has been slightly focused on cost, but it was not the main reason for the selection. Moreover, the software architecture exposed is modular and scalable, which allows the continuous improvement of the system.

Regarding the fast prototype, it has been a proof-of-concept of an embedded electronics system in an anti-stress ball to measure grip strength and walk time, among other measurements. The fast prototype uses the very same user-friendly interface of the conceptual design, allows the developer to track the status of the system over a serial debug line and the software architecture from the concept is maintained. The fast prototype has been implemented with low-cost off-the-shelf components that have been properly integrated into the anti-stress ball to some extent.

As a consequence of the lack of a compressive force calibration device in the laboratory premises, it has been required to design and develop an ad-hoc deadweight measurement device that has completely fulfilled the needs and expectations of this project. The calibration range of the deadweight measurement device is from 0 kgf to 40 kgf.

In the final stage of the project, it was detected that Fried's frailty criteria for weak grip strength could not be assessed with the anti-stress ball because Fried's table for grip strength was the result of using a Jamar hand-held dynamometer, which has a completely different shape than the anti-stress ball. And, since the way the force is applied to an object truly matters in the output result, Fried's table is not valid.

In overall, the requirements of the project have been fulfilled, but there are always related issues to work in the future. The first one is the design of the wireless power transfer charging system, which has been not accomplished fulfilled in this work. The next big challenge would be to design a second prototype including more features of the conceptual design such as the Bluetooth wireless communication, the battery integration and embedding the microcontroller unit into the anti-stress ball. In addition to that, the system may require an electromagnetic compatibility study as well as temperature simulations. Also, it would be great to test the fast prototype on adults and obtain a proper frailty criterion for the wearable device designed.

Finally, as a personal opinion, there have been some ups and downs during these months like in all projects; but, the work developed in the scope of the master thesis has clearly helped me to improve as an engineer and as a human being.

Bibliography

[1] Linda P. Fried, Catherine M. Tangen, Jeremy Walston, Anne B. Newman, Calvin Hirsch, John Gottdiener, Teresa Seeman, Russel Tracy, Willem J. Kop, Gregory Burke, Mary Ann McBurnie. "Frailty in Older Adults: Evidence for a Phenotype". *Journal of Gerontology: MEDICAL SCIENCES*, vol. 56A, no. 3, M146-M156, 2001.

[2] L. Dasenbrock, A. Heinks, M. Schwenk, J.M. Bauer. "Technology-based measurements for screening, monitoring and preventing frailty". *Zeitschrift für Gerontologie und Geriatrie*, Published Online, September 2016. DOI: 10.1007/s00391-016-1129-7.

[3] A. Chkeir, D. Safieddine, F. Chehade, J. Duchêne, D. Hewson, D. Bera, M. Collart, J.L. Novella, M. Dramé. "Is there a relationship between frailty indices and balance assessment in older people?". *2016 IEEE 18th International Conference on e-Health Networking, Applications and Services (Healthcom), Healthcom 2016*, 14-16 September 2016, Munich, Germany. DOI: 10.1109/HealthCom.2016.7749515.

[4] Takashi Yamada, Tomio Watanabe. "Development of grip strength measuring systems for infants". *2016 IEEE/SICE International Symposium on System Integration (SII), SII 2016*, 13-15 December 2016, Sapporo, Japan. DOI: 10.1109/SII.2016.7843988.

[5] P. Bustamante, K. Grandez, G. Solas, S. Arrizabalaga. "A low-cost platform for testing activities in parkinson and ALS patients". *2010 IEEE 12th International Conference on e-Health Networking, Applications and Services (Healthcom), Healthcom 2010*, 1-3 July 2010, Lyon, France. DOI: 10.1109/HEALTH.2010.5556550.

[6] Rana Jaber, David J. Hewson, Jacques Duchêne. "Design and validation of the Grip-Ball for measurement of hand grip strength". *Medical Engineering & Physics*, vol. 34, pp. 1356-1361, 2012. DOI: 10.1016/j.medengphy.2012.07.001

[7] Sunghoon Ivan Lee, Hassan Ghasemzadeh, Bobak Jack Mortazavi, Majid Sarrafzadeh. "A Pervasive Assessment of Motor Function: A Lightweight Grip Strength Tracking System". *IEEE Journal of Biomedical and Health Informatics*, vol. 17, no. 6, pp. 1023-1030, November 2013. DOI: 10.1109/JBHI.2013.2262833

[8] Fabrizio Vecchi, Cinzia Freschi, Silvestro Micera, Angelo M. Sabatini, Paolo Dario, Rinaldo Sacchetti. “Experimental Evaluation of Two Commercial Force Sensors for Applications in Biomechanics and Motor Control”. 2000 5th *International Functional Electrical Stimulation Society, IFESS 2000*, pp 390-393, Aalborg, Denmark.

[9] Shogo Kawaguchi, Kouki Nagamune. "An evaluation system of high risk factors for daily motions using force sensors". *2014 World Automation Congress, WAK 2014*, 3-7 August 2014, Waikoloa, USA. DOI: 10.1109/WAC.2014.6935974.

[10] J.M. Dias Pereira, Octavian Postolache, Vítor Viegas, Pedro Silva Girão. "A low cost measurement system to extract kinematic parameters from walker devices". *2015 IEEE International Instrumentation and Measurement Technology Conference (I2MTC), I2MTC 2015*, 11-14 May 2015, Pisa, Italy. DOI: 10.1109/I2MTC.2015.7151588.

[11] K. Grandez, P. Bustamante, G. Solas, I. Gurutzeaga, A. García-Alonso. "Wearable wireless sensor for the gait monitorization of Parkinsonian patients". *16th IEEE International Conference on Electronics, Circuits, and Systems, 2009, ICECS 2009*, 13-16 December 2009, Yasmine Hammamet, Tunisia. DOI: 10.1109/ICECS.2009.5410974.

[12] Pei-Chi Hsiao, Shu-Yu Yang, Bor-Shing Lin, I-Jung Lee, Willy Chou. "Data glove embedded with 9-axis IMU and force sensing sensors for evaluation of hand function". *2015 37th Annual International Conference of the IEEE Engineering in Medicine and Biology Society (EMBC), EMBC 2015*, 25-29 August 2015, Milan, Italy. DOI: 10.1109/EMBC.2015.7319426.

[13] David J. Hewson, Rana Jaber, Aly Chkeir, Ali Hammoud, Dhruv Gupta, Jennifer Bassement, Joan Vermeulen, Sandeep Yadav, Luc de Witte, Jacques Duchêne. "Development of a monitoring system for physical frailty in independent elderly". *2013 35th Annual International Conference of the IEEE Engineering in Medicine and Biology Society (EMBC), EMBC 2013*, 3-7 July 2013, Osaka, Japan. DOI: 10.1109/EMBC.2013.6610973.

[14] Keita Aoike, Kouki Nagamune. "Gait analysis with six axes inertial sensor and force sensor for daily motion". *2016 11th International Conference on Computer Science & Education (ICCSE), ICCSE 2016*, 23-25 August 2016, Nagoya, Japan. DOI: 10.1109/ICCSE.2016.7581549.

[15] J.M. Dias Pereira, Vítor Viegas, Octavian Postolache, Pedro Silva Girão. " Combining distance and force measurements to monitor the usage of walker assistive devices". *2017 IEEE International Instrumentation and Measurement Technology Conference (I2MTC), I2MTC 2017*, 22-25 May 2017, Turin, Italy. DOI: 10.1109/I2MTC.2017.7969673.

[16] Microchip Technology Inc.. "PIC24FJ128GA204 Family Data Sheet". Microchip Technology Inc., 2013-2015. [Online] Available: http://ww1.microchip.com/downloads/en/DeviceDoc/30010038c.pdf. [Accessed: 15 October 2017].

[17] Interlink Electronics. "FSR Integration Guide". Interlink Electroncis. [Online] Available: http://www.interlinkelectronics.com/integration_guides/FSR400Series_IG.zip. [Accessed: 15 October 2017].

[18] Freescale Semiconductor Inc.. "±2g/±4g/±8g Three Axis Low-g Digital Output Accelerometer Technical Data". Freescale Semiconductor Inc., 2007-2009. [Online] Available: https://www.nxp.com/docs/en/data-sheet/MMA7455L.pdf. [Accessed: 15 October 2017].

[19] Microchip Technology Inc.. "BM70/71 Bluetooth® Low Energy (BLE) Module Data Sheet". Microchip Technology Inc., 2015-2017. [Online] Available: http://ww1.microchip.com/downloads/en/DeviceDoc/60001372F.pdf. [Accessed: 15 October 2017].

[20] Microchip Technology Inc.. " SST25VF512 512 Kbit SPI Serial Flash Data Sheet". Microchip Technology Inc., 2011. [Online] Available: http://ww1.microchip.com/downloads/en/DeviceDoc/25076A.pdf. [Accessed: 15 October 2017].

Glossary

Table 43 - Glossary

Acronym	Meaning
ADC	Analog-to-Digital Converter
ASIC	Application-Specific Integrated Circuit
ASHT	American Society of Hand Therapists
BLE	Bluetooth Low Energy
BMI	Body Mass Index
CES	Center for Epidemiologic Studies
CESD-R	Center for Epidemiologic Studies Depression Scale Revised
CSn	Chip Select (active low)
FSR	Force-Sensing Resistor
GPIO	General Purpose Input Output
IMU	Inertial Measurement Unit
I2C	Inter-Integrated Circuit
I/O	Input/Output
IT	Information Technology
LED	Light-Emitting Diode
MCU	Microcontroller Unit
MISO	Master-In Slave-Out
MOSI	Master-Out Slave-In
PC	Personal Computer
PCB	Printed Circuit Board
RAM	Random-Access Memory
RGB	Red Green Blue

SCLK	SPI Clock
SI	International System of Units (from French, Système International d'únites)
SPI	Serial Peripheral Interface
TTL	Transistor-Transistor Logic
UART	Universal Asynchronous Receiver-Transmitter
USB	Universal Serial Bus
VCP	Virtual COM Port
WPT	Wireless Power Transfer